Acute regulation of synaptic NMDA receptor content in hippocampal neurons

Andrea L. McQuate

A dissertation

submitted in partial fulfillment of the

requirements for the degree of

Doctor of Philosophy

University of Washington

2017

Reading Committee:

Andres Barria, Chair

Jane M Sullivan, Chair

Rachel Wong

Program Authorized to Offer Degree:

Neuroscience

University of Washington

Abstract

Acute regulation of synaptic NMDA receptor content in hippocampal neurons

Andrea L. McQuate

Chairs of the Supervisory Committee:
Associate Professor Andres Barria
Associate Professor Jane M Sullivan
Physiology and Biophysics

Hippocampal-dependent learning, which is required for forming fact-based, declarative memories, involves changing the physical and functional characteristics of connections between neurons, called synapses. This process of "synaptic plasticity" is mediated by the *N*-methyl-D-aspartate receptor (NMDAR). NMDARs are ionotropic glutamate receptors found within synapses and when activated, initiate intracellular signaling cascades that result in plasticity. Historically, NMDARs have been considered static components of synapses. More recent evidence, however, overturns this dictum to reveal that NMDARs are dynamic, and regulated by many factors including receptor subunit composition and the previous activity of the neuron. In this thesis, I describe two means by which hippocampal neurons can regulate synaptic NMDAR content:

(1) The number and type of synaptic NMDARs can be regulated by a secreted glycoprotein, Wnt5a. Wnt5a increases the delivery of NMDARs into synapses from

intracellular compartments by triggering a signaling cascade involving membrane depolarization and release of calcium from internal stores.

(2) NMDARs can move laterally on the neuron surface between synaptic and extrasynaptic compartments in an activity-dependent, calcium-independent process.

The ability of neurons to finely tune their synaptic NMDAR content provides a means for optimizing the ability of a synapse to undergo plasticity given a certain set of conditions. The two mechanisms described here may provide potential platforms on which to develop novel therapeutics to treat neurodegenerative or neuropsychiatric disorders where synaptic plasticity has been compromised.

TABLE OF CONTENTS

LIST OF FIGURES

ACKNOWLEDGEMENTS

The input and support of many have gone into this dissertation work. Primarily, I would like to thank my (real) thesis advisor, Dr. Andres Barria, for his scientific expertise; not only in basic knowledge, but in the method, practice, and the elusive “science game.” I would also like to thank fellow lab mates, Ximena Opitz-Araya, Elena Latorre-Esteves, Alyx Bosworth, and Dr. Waldo Cerpa for their knowledge and time.

Second, I thank my committee members for supporting me throughout the duration of the thesis, even before most knew they would be committee members: Dr. Marc Binder, Dr. Marti Bosma, Dr. Jane Sullivan, and Dr. Rachel Wong. I especially want to thank Jane for stepping up into the position of Chair at the very last minute, when it came to light Andres wouldn’t be able to attend the defense.

Next, I thank my family for their eternal love and support: Mom, Dr. Giovonnae Anderson, Dad, Dr. David McQuate, and my sister and her husband, Dr. Sarah McQuate and Andrew Fabry. There are few people who would talk with me on the phone for over two hours about things that only matter to the elite force who are “the McQuates.”

My Seattle family has a significant part in this work as well as they cheered me on, inspired me, and put up with me (and I am not the easiest person to put up with): my roommate, Karen Ressler, partner in crime and Seattle mom Vivian Queija, and her husband Kevin Sanders, ARCS mom Carmen Gayton, writer friends Megan Cartwright, Maricar Calma, and Elizabeth Guizzetti. Last, for the chance to experience my research first-hand: Matt Hurst, Stanley Shikuma, Lika Seigel, all the members of Seattle Kokon Taiko. Hippocampus!

DEDICIATION

This thesis is dedicated to Ashiviska, the Sovereign Velna.

CHAPTER 1. INTRODUCTION

Neurons, the electrically excitable cells that compose the brain and nervous system, construct how we perceive our world and control how we act within it. The approximately hundred billion neurons of the human brain, once interconnected, manufacture our individual realties of who we each are, what we want, and why. This can be attributed in large part to the ability of these cells to encode information and form "memories," a process in which the synapse plays a major role.

The classic synapse consists of a site where the axon of a presynaptic neuron contacts the dendrite of a postsynaptic neuron, with a 20-40 nm synaptic cleft separating them. A single neuron can have thousands of postsynaptic sites distributed primarily across its dendrites, but also occasionally soma, and axons as well. Pre- and postsynaptic densities can be distinguished by the presence of respective specialized molecular structures that reflect the functions of each. Fundamentally, the synapse is not a passive connection that merely transmits information from one neuron to another, but can sculpt and bias this information in a manner governed by the properties of both the pre and postsynaptic molecular sites. Furthermore, a synapse's characteristics can change in the process known as "synaptic plasticity," with its gradual acquisition of a set of features thought to underlie new memory formation. **The work in this thesis aims to further clarify how synaptic plasticity is regulated at the molecular level.**

1.1 Synaptic plasticity is one form of memory acquisition.

The central hypothesis behind this principle, known as "Hebbian plasticity" after it was introduced by Donald Hebb in 1949, states that the strength of the synapse between a pre and postsynaptic neuron will increase if those neurons are active simultaneously. It is thought that each of the thousands of synapses on a neuron reaching an optimal weight, with some synapses

being stronger or weaker, constitutes learning, and the collective weights of those synapses, the memory "engram." This synapse-based form of information integration underlies the formation of long-lasting memories and will be the basis of this thesis.

1.2 The hippocampus is vital for the initial acquisition of memory.

A seahorse shaped structure located bilaterally deep in the medial temporal lobe, the hippocampus is vital for the initial formation of new memories [1], navigation, and spatial learning [2]. Recent evidence points to the dorsal and ventral areas of the hippocampus having separate memory encoding functions, with the dorsal hippocampus involved in cognitive information processing, while the ventral hippocampus is primarily emotional in function [3]. Lesions to the hippocampus can result in anterograde amnesia, or the inability to learn new information, whether cognitive or emotional. It also has been demonstrated that in neurodegenerative disorders, abnormalities first begin within hippocampal synapses, even before the onset of noticeable symptoms [2, 4].

1.3 The hippocampus is an ideal experimental paradigm.

The clearly defined architecture and neuronal connections within the hippocampus, as well as the ability of hippocampal slices to stay alive in culture, makes it an ideal experimental paradigm, with obvious ramifications for understanding the cellular mechanisms underlying memory (Figure 1.1). The hippocampus has three major sub-regions of cells: the dentate gyrus (DG), CA1, and CA3 (CA for Cornu Ammonis, or Ammon's horn).

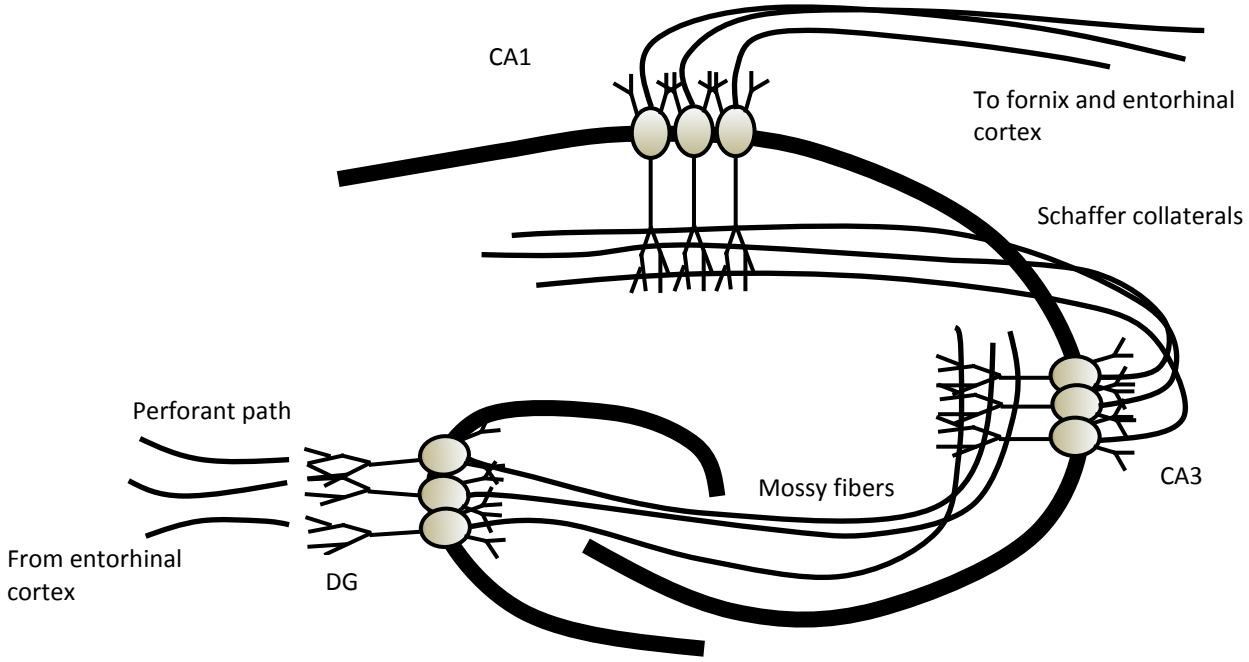

Figure 1.1 The structural anatomy of the hippocampus and the trisynaptic circuit. Input from entorhinal cortex synapses onto neurons in dentate gyrus (DG) via the perfornat path. DG neurons then project axons onto CA3 neuron dendrites via the mossy fibers. CA3 neurons then send their axons to dendrites of CA1 neurons via the Schaffer collaterals.

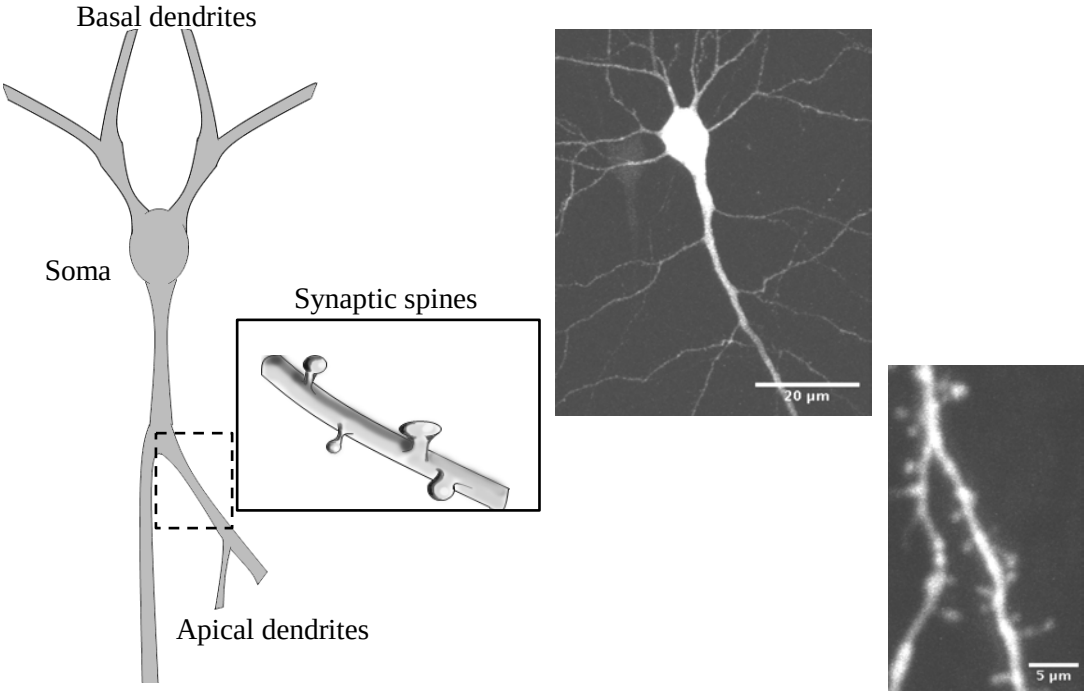

Figure 1.2 Morphology of CA1 neuron and its spines. (Left) Structure of CA1 neuron in hippocampus and of synaptic spines (inset). (Right) Example pictures of CA1 neuron (top) and its spines (bottom) overexpressing green fluorescent protein (GFP). Taken via two-photon microscopy from a biolistically transfected hippocampal slice. Scale bar for neuron = 20 µm. Scale bar for spines = 5 µm.

Pyramidal cells in these three areas have a distinct morphology, with apical and basal dendrites extending bilaterally from the soma (Figure 1.2, left). Sensory input arrives to the hippocampus from the entorhinal cortex through either direct or indirect pathways. In the direct pathway, neurons from entorhinal cortex synapse onto the distal ends of pyramidal neurons in all three hippocampal areas. In the indirect pathway, input from the entorhinal cortex enters the hippocampus and is processed through a trisynaptic circuit: first, information synapses onto cells in the dentate gyrus via the perforant path. Neurons from the dentate gyrus send their axons to neurons in CA3 via the mossy fibers. The axons of CA3 neurons project to the proximal area of CA1 neuron apical dendrites via the Schaffer collaterals. CA1 neurons then project axons to the fornix, which is the major output of the hippocampus, and back to entorhinal cortex. Both the hippocampal direct and indirect pathways have been shown to be important for learning and memory, though the precise role each plays in the process and the amount of overlap they share warrant further investigation.

The axons in these synaptic connections release the fast, excitatory neurotransmitter glutamate, which elicits excitatory currents in their respective postsynaptic neurons by binding glutamate-specific receptors. Postsynaptic sites primarily consist of spines, which are small (~1 μm) mushroom shaped protrusions extending from the postsynaptic dendrite (Figure 1.2, left, inset). The spines contain much of the postsynaptic molecular machinery required to process synaptic information. The work in this thesis concerns the CA3-CA1 hippocampal synapse, which has been shown to have a unique role in learning (see Section 1.5).

1.4 Hippocampal synaptic plasticity underlies new memory formation.

Fundamentally, each of the aforementioned synapses in the hippocampus change their functional and morphological properties in response to sensory information. What mechanisms

translate sensory cues into long-lasting changes in synaptic properties, and hence, new memories? In 1973, it was demonstrated that a strong tetanus to axons of the perforant pathway strengthen synaptic connections between the entorhinal cortex and the neurons of the DG—that is, the response of the postsynaptic DG neuron to a test stimulus of the same magnitude was larger following tetanic stimulation of the perforant pathway than prior to it [5]. This form of experimentally induced plasticity, known as long-term potentiation or LTP, persists for hours following the tetanus, a hallmark of memory that long outlasts the duration of the stimulus. Similarly, weak but persistent stimulation of axons in the Schaffer collaterals results in long-term depression (LTD) at the CA3-CA1 synapse [6, 7]. These experimental paradigms quickly became regarded as a molecular form of memory that warranted extensive investigation.

1.5 NMDA receptors coordinate synaptic plasticity.

There are two general classes of ionotropic glutamate receptors at the postsynaptic site: α-amino-3-hydroxy-5-methyl-4-isoxazolepropionic acid receptors (AMPARs) and N-methyl-D-aspartate receptors (NMDARs). Both receptors are excitatory, meaning they have a reversal potential above the resting membrane potential, and when activated, will pass positive ions into the cell and raise the membrane potential closer to a firing threshold. However, the two receptors play different roles in synaptic plasticity: NMDARs are necessary for plasticity *induction*, while AMPARs mediate its *expression*. Historically, the NMDAR is considered the "static" molecular coordinator of this process by regulating the number of AMPARs expressed in the synapse [7]. Higher numbers of AMPAR at the synapse translates to a "stronger" synapse, and lower numbers, a "weaker" synapse. Although NMDARs share the same topology as the AMPAR, they are fundamentally different for two reasons:

(1) NMDARs only open once they have bound glutamate *and* the postsynaptic neuron is sufficiently depolarized. The ability of NMDARs to activate selectively during times of postsynaptic depolarization emerges from a magnesium (Mg^{2+}) plug in the receptor pore that prevents ion flux, which is only released by a rise in the membrane potential. This makes the NMDAR a coincidence detector for simultaneous pre (glutamate binding) and post (membrane depolarization) synaptic activity, and serves to mark when two neurons are active at the same time. These properties make them molecular coordinators of Hebbian plasticity, and have brought them to the forefront of research as a means of studying the molecular basis of memory.

(2) Upon activation, NMDARs pass calcium, carrying roughly 10% of the NMDAR mediated charge influx [8]. Calcium is the initiator of many intracellular signaling cascades, and is well-documented in neurons as one of the major factors of synaptic plasticity. In the "classic" view of synaptic plasticity in hippocampus, when NMDARs are activated, they initiate plasticity cascades proportionate to the amount of calcium influx. High levels of activation and thus high calcium influx activate calmodulin and the enzyme CaMKII, leading to phosphorylation of proteins ultimately promoting AMPAR trafficking into synapses [9, 10]. These modifications functionally "strengthen" the synapse, and results in LTP.

Meanwhile, when NMDARs are weakly activated, the lower calcium influx activates phosphatases such as PP2 and ultimately instigates AMPAR removal, thus resulting in long-term depression (LTD). In these models, a high frequency stimulus delivered to afferent axons produces a long-lasting increase in the AMPAR mediated EPSC (excitatory postsynaptic current), while a low-frequency stimulus decreases the AMPAR EPSC [7], though it may be the precise pattern of stimulation and calcium influx that determines the direction of plasticity, rather than the absolute calcium level [11]. Stimulation of NMDARs is also accompanied by corresponding changes in

spine morphology, with LTP associated with an increase in the spine size, and LTD, a decrease [12].

NMDARs are fundamental for plasticity particularly at the CA3-CA1 synapse. Delivering a NMDAR antagonist (such as APV) to the hippocampus completely disrupts LTP at this synapse [13, 14]. Furthermore, in a more careful evaluation of NMDAR's role specifically in this region, genetic manipulations that specifically remove NMDARs from CA1 neurons also blocks LTP [15]. Although the mRNA for NMDARs is equally disseminated in CA3 and CA1 regions of the hippocampus, there is higher NMDAR protein expression in CA1[16]. The strong presence of the NMDAR at this synapse and its unique physiological properties give the CA3-CA1 synapse three attributes that underscore its importance to memory formation:

(1) Cooperativity: potentiation requires strong activation of the Schaffer collaterals in order to relieve the Mg^{2+} plug and activate NMDAR, and thus weak, irrelevant stimuli are disregarded.

(2) Input specificity: Only synapses where NMDAR have bound glutamate released by a presynaptic neuron will undergo potentiation.

(3) Associativity: Depolarization initiated by a strong input to some synapses may spread to weaker synapses where NMDAR have bound glutamate and potentiate those in tandem [17].

These properties make the NMDAR and the ion flux through them imperative for the proper induction of synaptic plasticity and memory formation (but see Section 1.9).

1.6 NMDARs exist as obligate heterotetramers.

NMDARs consist of four subunits, arranged as a "dimer of dimers." Each dimer is composed of one essential GluN1 subunit and one regulatory GluN2-3 subunit. GluN1 subunits

bind glycine and are fundamental for proper NMDAR trafficking. Although splice variations of GluN1 subunits have been described, these subunits are relatively homogenous compared with their GluN2 counterparts. The GluN2 subunits bind glutamate, and can be further subdivided into GluN2A-D subtypes that are encoded by four distinct genes. These subunits are each expressed in distinct regions of the brain, including neocortex, striatum, and hippocampus [18-20]. Of these types, GluN2A- and GluN2B-containing receptors are highly expressed in hippocampus and therefore studying their interplay has become of primary importance for studying molecular memory.

GluN2A and GluN2B-containing NMDARs have different biochemical structures, which confer distinct physiological characteristics and roles in plasticity: fundamentally, receptors that contain primarily GluN2A subunits have a high affinity for glutamate, greater channel open probability, and fast deactivation kinetics [21]. In contrast, receptors that contain primarily GluN2B subunits demonstrate a lower opening probability and slower channel kinetics. NMDARs containing both subunits are inserted into synapses via vesicle fusion in a process accelerated by protein-kinase C (PKC) dependent phosphorylation of SNAP25, a member of the SNARE family of fusion proteins [22]. Additionally, both receptor subunits have a four-amino acid (ESDV) PDZ-binding domain that interacts with membrane associated guanylate kinases (MAGUKs), such as PSD protein of 95 KDa (PSD-95) and synapse-associated protein 102 (SAP-102) to localize the subunits to synaptic sites. Phosphorylation of the serine residue in the ESDV motif promotes dissociation from postsynaptic proteins and removal of receptors from the synapse [23].

However, receptors that contain GluN2A versus GluN2B subunits demonstrate different trafficking patterns. GluN2A-containing receptors require activity, agonist binding [24]

or intracellular calcium [25] to drive them into synapses. Once incorporated, they remain relatively stable in the postsynaptic density. GluN2B-containing receptors, in contrast, constitutively move into synapses and then are removed [24]. This is governed by an additional motif in the GluN2B C-terminus (YEKL), adjacent to the ESDV motif, which allows receptors to interact with the AP2 adaptor complex, leading to clathrin-mediated endocytosis. Once internalized, GluN2B subunits co-localize with proteins involved in endosome recycling, fating their return to synapses [26].

In further contrast, the C-terminus of GluN2B-containing receptors directly associates with the active form of CaMKII, and mutations of this region of the GluN2B C-terminus compromise synaptic plasticity. GluN2A, meanwhile, does not bind CaMKII [27]. This association may also selectively promote GluN2B internalization, since active CaMKII can activate the enzyme casein kinase 2 (CK2), which selectively phosphorylates S1480 in the ESDV motif in GluN2B subunits, which destabilizes GluN2B interaction with MAGUK proteins. [28, 29].

Some evidence points to these two subunits having different roles in plasticity. GluN2A subunits have been demonstrated as necessary to induce LTP, and GluN2B subunits necessary for LTD [30, 31]. If there is a distinction for these subunits in plasticity, however, it may depend on the precise on the age of the animals used for the preparation, or on the concentrations and specificity of antagonists used. Further studies show that in older animals, the presence of the GluN2B subunit C-terminus is enough to allow LTD induction, independent of ion flux through the channel, and that the C-terminus of GluN2A subunits decreases the potential for LTP [32]. In general, however, the strict association of each NMDAR subunit with forms of plasticity has not proved reproducible [33]. This points towards a more complicated picture of how NMDAR

subunit composition regulates plasticity, and a greater need to evaluate in detail how each of these subunits contributes to memory formation.

1.7 While NMDARs govern plasticity, the subunits they contain may govern metaplasticity.

"Metaplasticity," or the "plasticity of plasticity," describes the ease by which a synapse can change its properties. According to Hebbian plasticity, should two interconnected neurons fire at the same time, the strength of the synapse between them will increase in a "boundless" manner. Neurons have limited firing rates, however, and boundless synaptic strengthening could result in saturation and eventual loss of information. New learning rules have hence been developed, which include a plasticity threshold that shifts according to the history of the synapse. Thus, at a synapse that has already been potentiated, the threshold for subsequent potentiation increases [6, 34, 35].This theory of a shifting threshold for plasticity was developed by Bienenstock, Cooper and Monroe for neurons visual cortex in 1982 [34], and has been further experimentally demonstrated in hippocampus [6]. The observation that on CA1 neurons, smaller synaptic spines are more likely to undergo plasticity than larger spines provides further evidence towards the existence of metaplasticity in the hippocampus [12].

GluN2B-containing NMDARs demonstrate slow deactivation kinetics, allowing ample calcium influx and the subsequent activation of downstream effectors [21]. In addition, they form associations with active CaMKII, increasing the efficiency for plasticity [27]. These properties have given NMDARs containing GluN2B subunits a unique role for "easing" the ability of synapses to undergo plasticity. Toward this end, it has been shown that GluN2B overexpression increases spine mobility, while GluN2A enhances their stability [36]. The GluN2A/GluN2B ratio can therefore be used as a metric for metaplasticity [37].

The primary evidence that the GluN2A/GluN2B ratio impacts a plasticity threshold emerges from studies of the critical period of development in visual cortex. The critical period is window of time early in the postnatal life of an organism, between 1-3 weeks after birth, where new synaptic connections are established and unnecessary ones pruned [37]. Evidence in neuronal synaptosomes prepared from neurons in visual cortex show that during this time, protein levels of GluN2B begin high after birth, while levels of GluN2A begin low and gradually increase [38-40]. This is accompanied by an increase in the LTP threshold and has been deemed the GluN2B to GluN2A "switch." Activity is essential: dark-rearing animals results in a persistently lower GluN2A/GluN2B ratio and decreased synaptic efficiency [38]. This switch during the critical period of development has been demonstrated in a variety of preparations from across the brain, including the hippocampus [37, 41].

1.8 GluN2B/GluN2A switch may reflect a more universal synaptic plasticity process beyond development.

Evidence exists that the adult brain maintains the ability to shift the GluN2A/GluN2B ratio in synapses on an acute basis in response to activity. When dark-reared animals are exposed to light at a later age, the sensory information initiates the same GluN2B to GluN2A switch in visual cortex that would occur during the critical period of a normally developing animal within two hours [42]. Furthermore, animals that were normally reared and then brought into a dark environment for an extended period will demonstrate the reverse—a decrease in the GluN2A/GluN2B raito. Lastly, this shift can be imparted rapidly *in vitro.* Inducing LTP in a hippocampal slice increases the speed of the global NMDAR EPSC in CA1 neurons, indicating an increase in the number of GluN2A-containing receptors [43]. In contrast, inducing LTD slows the decay time constant, indicating the presence of GluN2B-containing NMDARs at the synapse. The

maintenance of intracellular pathways that govern this switch may be crucial for the adult brain to continue incorporating new information into a limited number of neurons and synapses.

1.9 New roles of NMDARs in plasticity are constantly emerging.

NMDARs and their roles in synaptic plasticity have been studied for decades, yet new postulates are constantly emerging regarding their functions. Some studies suggest that in addition to promoting AMPAR insertion into synapses, tonic calcium through NMDARs can also suppress AMPAR trafficking, with differential roles of GluN2A and GluN2B subunits; GluN2B-containing receptors restrict the formation of new synapses, while GluN2A-containingreceptors restricts existing synapses from strengthening [44, 45]. New evidence suggests that NMDARs have a metabotropic function, and do not require opening of the pore or calcium influx to induce LTD [46], although these findings have raised contention [47]. These metabotropic NMDAR functions in LTD have also been shown to correlate with structural LTD and decreases in spine size [48]. The metabotropic effects may be attributable to a conformational change in the NMDAR C-terminus that occurs upon agonist binding, which leads to a re-localization of CaMKII and synaptic depression [49, 50]. These “new” roles for NMDARs underscore the complexity of their signaling, and the need for more careful evaluation of their properties.

1.10 NMDARs are highly implicated in neurological disorders.

Given their role coordinating synaptic plasticity, NMDAR function drastically impacts learning and the incorporation of new memories. Dysregulation of NMDAR function is implicated in many neuropsychiatric and neurodegenerative disorders, including addiction, schizophrenia, and Alzheimer’s disease. These dysregulations include detrimental decreases in NMDAR function, which would reduce the ability of synapses to undergo plasticity. In Alzheimer’s disease, for example, an age-dependent neurodegenerative disorder involving memory loss and cognitive

impairments, toxic amyloid-beta signaling leads to eventual NMDAR endocytosis and removal from synapses [51]. Furthermore, GluN2B-containing NMDAR function is compromised in an Alzheimer's disease mouse model [52].

At the same time, calcium passed by NMDARs could be cytotoxic, especially as calcium buffering and handling in aging neurons is compromised [53, 54]. In Alzheimer's disease, synapse degeneration and calcium mishandling in CA1 neurons appear before onset of visible symptoms [4]. Strikingly then, one might expect that the removal of NMDARs could be therapeutic. In fact, one of two drugs currently on market for Alzheimer's disease, memantine, is a partial NMDAR antagonist, designed to reduce calcium influx through the receptors and ameliorate potentially cytotoxic effects [55]. The fact that memantine blocks activity through the very receptors that are crucial for memory formation, already compromised in Alzheimer's disease, speaks to the complexity of this disorder and need for a deeper understanding of NMDAR function and how it becomes dysregulated.

1.11 NMDARs are not static.

Historically, NMDARs have been considered static components of synapses, while AMPARs dynamically move in and out. This hypothesis was based on evidence of silent synapses that contain NMDAR but not AMPAR, until stimulation promotes AMPAR trafficking to the synapse [56], and from the observation that NMDARs are often found in complex with large signaling platforms and scaffolding proteins that might hinder movement [7].

Closer evaluation of previous work, however, suggests that NMDARs are as dynamic as their AMPAR counterparts. For example, long-term pharmacological inhibition of neuronal activity promotes NMDAR expression on the surface of dissociated neurons [57] and promotes phosphorylation of receptors in a manner consistent with forward trafficking [58]. In an

electrophysiological paradigm, withdrawing stimulation for a short period increases the size of the evoked NMDAR EPSC [59]. Meanwhile, increased concentrations of calcium inside cells yields NMDAR rundown via actin depolymerization [60, 61], and promotes NMDAR inactivation [62]. An NMDAR-based LTP (a long term potentiation of NMDAR currents) in the mossy fiber to CA3 synapse has been described, requiring the release of calcium from intracellular stores [63]. Similarly, stimulation of metabotropic mGluR5 receptors and the release of calcium from internal stores has been shown to be necessary for the acute GluN2B to GluN2A switch observed in hippocampal slice preparations [25]. Collectively, these experiments suggest that activity and increases in intracellular calcium, whether from the stores or from the extracellular space, modulate NMDAR.

1.12 What mechanisms regulate NMDAR dynamism remain unclear.

What precise molecular cascades translate neuronal activity or calcium levels into NMDAR functional changes? Are there extracellular signals besides activity that can modulate NMDAR function, and how? What signaling components, such as intracellular calcium, are important for different aspects of NMDAR dynamism? Lastly, what cellular mechanisms are in place to govern the subunit composition of NMDARs within synapses? The answers to these questions are in large part currently unexplored.

Although there are potentially many ways of regulating NMDAR function, this thesis will focus on “acute” receptor movement at two different timescales: trafficking of new NMDAR into postsynaptic sites, which can occur within hours, or the lateral movement of receptors already on the surface between synaptic and extrasynaptic spaces, which occurs on a minute-by-minute basis. This thesis uses a combination of electrophysiology, functional imaging, and calcium imaging to (1) decipher a molecular pathway initiated by an extracellular protein that promotes

NMDAR trafficking into hippocampal synapses, (2) determine whether NMDARs can move laterally between hippocampal synaptic and extrasynaptic spaces, and (3) evaluate the role of NMDAR subunit composition in both of these. These experimental aims will be further detailed in the following two chapters:

Chapter Two: A novel neuronal Wnt/calcium signaling cascade regulates NMDAR trafficking

Wnts are secreted glycoproteins heavily implicated in the developing nervous system, where they carry out well-characterized roles in axon-pathfinding, synaptogenesis, and dendritic arborization via canonical and non-canonical pathways. Wnt expression and secretion, however, also continue postnatally, and persist throughout the lifetime of the adult. The purpose and the dynamics of non-embryonic Wnt signaling have yet to be extensively characterized.

Previously, we have shown that Wnt5a specifically and acutely upregulates NMDAR EPSCs in mature hippocampus [64]. This effect depends on the tyrosine kinase-like receptor specific for Wnt5a, RoR2, which is highly expressed in hippocampus [65]. The mechanisms behind this Wnt5a-induced NMDAR potentiation, however, are unknown. In this chapter, I will describe the molecular pathway whereby Wnt5a increases the delivery of NMDARs containing the GluN2B subunit into synapses. This pathway includes membrane depolarization, release of calcium from intracellular stores, and the subsequent SNARE-dependent trafficking of GluN2B-containing NMDARs into synapses. It is possible that by increasing NMDAR delivery, Wnt5a facilitates the reorganization of synapses that occurs during adult learning.

<u>Chapter Three:</u> Dynamic, lateral exchange of synaptic and extrasynaptic NMDARs

In the third chapter, I describe how NMDARs can move laterally between synaptic and extrasynaptic compartments. While it has been demonstrated that NMDARs are quite mobile in dissociated hippocampal neurons, their ability to move in more intact paradigms such as the hippocampal slice has been under debate, and it is unclear whether this occurs *in vivo*. I have shown that following blockade of synaptic NMDARs, responses can recover up to 73% of the original baseline, suggesting that this lateral movement in hippocampal slices exists. This exchange was found to be activity dependent, but did not require intracellular calcium. In addition, this exchange depended on the subunits the receptor contained.

Both aspects of NMDAR mobility described here can directly control the number and type of NMDA receptors in the synapse, can shape the NMDAR-mediated EPSC, and therefore may have profound consequences for synaptic plasticity. Understanding NMDAR mobility, therefore, has applicability to many neurodegenerative disorders, learning, and memory.

CHAPTER 2

A novel neuronal Wnt/calcium signaling cascade regulates NMDAR trafficking

2.1 Introduction

Wnt signaling comprises a multigene family of secreted glycoproteins that can bind multiple types of receptors, including Frizzled, Ror, and Ryk receptors, to initiate a wide variety of intracellular signaling cascades that regulate the embryonic development of metazoans [66, 67].

While Wnt signaling has been studied intensely in embryonic development and cancer, it is poorly understood in the postnatal brain. Wnt ligands and Wnt receptors continue to be expressed postnatally, suggesting Wnt signaling cascades might also play a part in neuronal maintenance and synaptic function beyond embryonic development [68, 69]. The potential role of Wnt signaling in proper brain functioning is further underscored by the implication of Wnt signaling elements in several neuropathologies including schizophrenia [70], bipolar disorder [71], and Alzheimer's disease (AD)[72], where deregulation of Wnt signaling has been proposed as an etiological cause [73, 74] and become a novel molecular target in AD therapeutics [73]. However, it is not known which Wnt signaling cascades exist and operate in mature neurons, nor what their role is.

The best understood Wnt signal transduction cascade is the canonical Wnt/ß-catenin pathway that controls gene transcription during development. Canonical Wnt ligands bind a Frizzled receptor and the co-receptor LRP6 (low-density lipoprotein receptor-related protein) to initiate a signaling cascade that stabilizes cytosolic ß-catenin allowing its translocation to the nucleus where it binds transcription factors and alters gene expression. Within a homeostatic range, canonical ß-catenin-dependent signaling regulates cell proliferation and promotes cell survival

during development and regeneration [66, 75]. It is well-documented that alterations in this pathway lead to cancer or developmental abnormalities [75, 76].

Less understood are the ß-catenin independent or noncanonical pathways that may intersect with numerous other intracellular signaling cascades depending on cell-type and Wnt receptor context [67, 77]. Historically, noncanonical signaling has been divided into the Wnt/Ca^{2+} and Wnt/planar cell polarity pathways although there is marked crosstalk between the two cascades. Noncanonical Wnt ligands mediate the induction of intracellular Ca^{2+} transients during embryonic development that are necessary for proper dorsal-ventral patterning and direct body axis specification [78, 79]. Studies in cells of the enveloping layer of zebrafish blastulae [80] or *Xenopus* embryos [81, 82] also indicate that noncanonical Wnt signaling may involve intracellular calcium release to activate protein kinase C (PKC) and calcium/calmodulin-dependent protein kinase II (CaMKII). The planar cell polarity pathway, first studied in *Drosophila*, activates monomeric GTPases Rho and Rac, which in turn activate Jun-N-terminal kinase (JNK), ultimately restructuring the cytoskeleton to organize the bristles and hairs of the *Drosophila* cuticle [83]. In both forms of noncanonical Wnt signaling, intracellular calcium appears to be an important downstream signaling messenger. However, the signaling cascade leading to an increase in intracellular Ca^{2+}, as well as its source and dynamics remain unknown. Importantly, it is not known whether noncanonical Wnt/Ca^{2+} signaling is present in mature neurons and whether it plays a role in regulating neuronal function.

The expression of both canonical and non-canonical Wnt ligands continues throughout the lifetime of the adult, but their precise function in the mature nervous system has yet to be fully explored. Particularly, Wnts appear to play a role in synaptic maintenance, function, and plasticity [69]. The canonical Wnt ligand Wnt7a, promotes vesicle release, decreases paired pulse

facilitation, and may have a role during synaptic remodeling in hippocampus [84, 85]. Compromised Wnt7a signaling is associated with a general decrease in synaptic strength in hippocampus [85].

In contrast, the non-canonical ligand Wnt5a appears to have a primarily postsynaptic function in the adult hippocampus. Wnt5a has been shown to promote clustering of PSD-95 at synapses of dissociated hippocampal neurons through the enzyme JNK [86], and can lead to a rapid calcium increase in hippocampal dendrites, though the mechanism behind this increase is unclear [87]. It is likely mediated by a neuronal form of the Wnt/Calcium signaling cascade present during embryonic development.

We have previously found that Wnt5a rapidly upregulates synaptic NMDAR currents, and subsequently can facilitate the induction of synaptic plasticity [64]. Because NMDARs are the coincidence detectors for simultaneous pre and postsynaptic activity and are fundamental for learning and synaptogenesis, understanding how non-canonical Wnt lignads regulate synaptic NMDARs is of critical importance.

Here, we investigated the molecular mechanisms by which Wnt5a potentiates NMDAR currents in hippocampus. We report that Wnt5a depolarizes neurons and mobilizes calcium from intracellular stores to increase SNARE-dependent trafficking of NMDARs. This novel non-canonical Wnt signaling pathway requires tyrosine kinase-like orphan receptor 2 (RoR2), activation of phospholipase C, and the participation of voltage-gated calcium channels. Our results demonstrate that Wnt/Calcium signaling can regulate the presence of NMDARs at synapses, particularly those containing GluN2B subunits, suggesting a novel role for Wnt signaling in the postnatal brain.

2.2 Materials and methods

Hippocampal slices

Organotypic hippocampal slices (400 μm thick) were prepared according to standard procedures from postnatal day (P)6-9 male and female Sprague Dawley rats and maintained in culture for 3-8 days at 35°C [88]. Animals were handled in accordance with University of Washington (Seattle, WA) institutional animal care and use committee guidelines.

Dissociated neurons

Cultured hippocampal neurons were obtained by dissecting hippocampi from p1-2 Sprague Dawley males and female rats. Primary neurons were plated onto glass coverslips coated with poly-d-lysine and maintained in Minimal Essential Medium (Gibco) containing 10% horse serum, 2% B27, 2.5% HEPES, 0.8% glucose, 1% sodium pyruvate, 1% glutaMAX, 1% Pen/Strep. After four days in culture, 2 mg/mL 5-fluoro-2'deoxyuridine and 5 mg/mL uridine were added to the medium to suppress glial growth. Cells were used in experiments 1-2 weeks after plating.

Wnt constructs

Wnt5a, Wnt7a, or a control empty vector containing no Wnt ligand were expressed in HEK-293 cells for 72 hours. Conditioned medium containing Wnt proteins was harvested and centrifuged at 1000 rpm for 5 min. The supernatant containing Wnt ligands (~20 mL) was collected and dialyzed against 2 L artificial CSF (ACSF) without calcium for 16-24 hours (Spectra/Por 4 Dialyzer Tubing, molecular weight cutoff 12-14 KDa; cat no. 3787D40; Thomas Scientific) at 4°C. For electrophysiological experiments, Wnt constructs were further diluted 1/3 with fresh ACSF at the time of the experiment. All Wnt constructs and conditioned media controls were used within 4 days post dialysis.

Calcium imaging

Cultured dissociated neurons were loaded with 3 μM Asante calcium red in neuronal medium at room temperature for 30-45 min, then incubated in neuronal medium without indicator for an additional 30-45 min. to allow intracellular hydrolysis of the AM ester. For experiments, neurons were perfused with ACSF containing (in mM) 10 Glucose, 2.5 KCl, 118 NaCl, 1 NaH2PO4, 2 CaCl2, 2 MgCl2, 26 NaHCO3, pH 7.4, bubbled with 95% O2, 5% CO2 and imaged at room temperature on a 510 Meta Confocal (Zeiss) at 543 nm using a 63X water immersion objective. Mean fluorescence was measured and background subtracted using ImageJ. The analysis was repeated for 2-3 dendrites and averaged for each cell.

Electrophysiology

CA1 neurons from organotypic hippocampal slices were recorded in modified ACSF containing (in mM) 10 Glucose, 2.5 KCl, 118 NaCl, 1 NaH2PO4, 2 CaCl2, 2 MgCl2, 26 NaHCO3, pH 7.4. In the SNAP25 experiment (Fig 2.4E) 4 CaCl2 and 4 MgCl2 was used. The bath temperature was kept between 22.8-23.0°C. CA1 neurons were patched under visual guidance with glass pipettes (~3-4 MΩ) filled with either a cesium based (in mM 115 CsMeSO4, 20 CsCl2, 10 Hepes, 2.5 MgCl2, 4 MgATP, 0.4 Na3GTP, 10 Na-phosphocreatine, 0.6 EGTA, pH 7.25) or K^+-based (115 K-gluconate, 20 KCl, 10 Hepes, 2.5 MgCl2, 4 MgATP, 0.4 Na3GTP, 10 Na-phosphocreatine, 0.6 EGTA, pH 7.25) internal solution depending on the experiment. Recordings were obtained with a MultiClamp 700B amplifier (Axon Instruments) and pClamp 10.1 software.

NMDAR-mediated currents were recorded in the presence of 2 μM 2-chloroadenosine, 2 μM NBQX, and 100 μM picrotoxin from hippocampal neurons voltage-clamped at +40mV. A

bipolar cluster electrode (CE2C55, FHC) was placed on the Schaffer collaterals about 100 μm from the CA1 cell of interest and responses evoked at 0.1 Hz.

Imaging

Primary hippocampal neurons were transiently transfected with GluN2B-SEP and equimolar GluN1-untagged, to ensure proper receptor assembly and trafficking [24] using Lipofectamine LTX (Invitrogen). Dissociated neurons were imaged on a confocal microscope (Zeiss 510 Meta). Images were taken every five minutes. Each image was a z-stack of 7-9 1μm planes, and then projected for maximum intensity. At the end of the experiment, pH sensitivity of the construct was confirmed with an impermeant low pH ACSF (pH=5.5) containing MES hydrate instead of sodium bicarbonate. Mean integrated fluorescence density was measured and background subtracted using ImageJ. The fluorescence of 1-2 dendrites was measured and then averaged for each cell.

Knockdown of RoR2.

SureSilencing shRNA plasmids from SABiosciences (cat. no, KR55098G) targeting rat RoR2 sequence (NM001107339) described elsewhere [65] were transfected via Lipofectamine LTX (Invitrogen) into dissociated hippocampal neurons 48 hours prior to experimentation.

Statistics

Statistical significance was determined using a Student's standard paired and unpaired t-test. Where appropriate, one-way ANOVA was used with Tukey's Multiple Comparison test. A p value of < 0.05 was considered statistically significant.

Chemical reagents

2-cholorodenosine was purchased from Sigma-Aldrich. All other reagents used were purchased from Tocris. Preparation of drugs followed company specifications. When drugs were dissolved in DMSO, the total DMSO concentration in the bath was <0.2%.

2.3 Results

2.3.1 Wnt5a mobilizes intracellular Ca^{2+} to potentiate synaptic NMDAR currents.

To examine whether Wnt ligands signal via the noncanonical Wnt/Ca^{2+} pathway in mature neurons, dissociated hippocampal neurons were loaded with the calcium indicator Asante Calcium Red (ACR), which can be easily loaded into neurons and is sensitive to small changes in Ca^{2+} (K_d = 400 nM). We added either a canonical ligand, Wnt7a or, noncanonical Wnt ligand, Wnt5a to the perfusate. At the end of the experiment, ACSF containing high KCl (50 mM), which depolarizes neurons and subsequently activates voltage gated calcium channels, was added to the bath as a positive control. Bath application of Wnt5a significantly increased intracellular Ca^{2+} in neuronal dendrites 32 ± 12% above baseline ($p < 0.05$), while Wnt7a did not (Figure 2.1A and B). Control medium containing no Wnt ligand also did not affect intracellular Ca^{2+} (not shown). To further confirm the specificity of the calcium rise to Wnt5a, we knocked down a putative Wnt5a receptor in hippocampus. RoR2. RoR2 is a tyrosine kinase-like receptor we have shown to be highly expressed in CA1 and is required for the Wnt5a-mediated increase in NMDAR amplitudes [65]. Transfecting neurons with an shRNA targeting the RoR2 receptor eliminated Wnt5a's ability to increase intracellular levels of calcium (Figure 2.1C and D).

Two complementary experiments were designed to investigate the Ca^{2+} source contributing to the cytoplasmic Ca^{2+} rise. First, neurons were perfused with nominally Ca^{2+} free ACSF. Wnt5a still significantly raised cytoplasmic Ca^{2+} 13 ± 3% above baseline ($p < 0.005$, Figure 2.2A), though

the response did not have the same kinetics or amplitude as when extracellular Ca^{2+} was present. We then tested the role of intracellular Ca^{2+} stores by preincubating the neurons for 30 minutes with cyclopiazonic acid (CPA), an inhibitor of the SERCA pump, which prevents store refilling [89]. CPA was also maintained in the bath during the experiment.

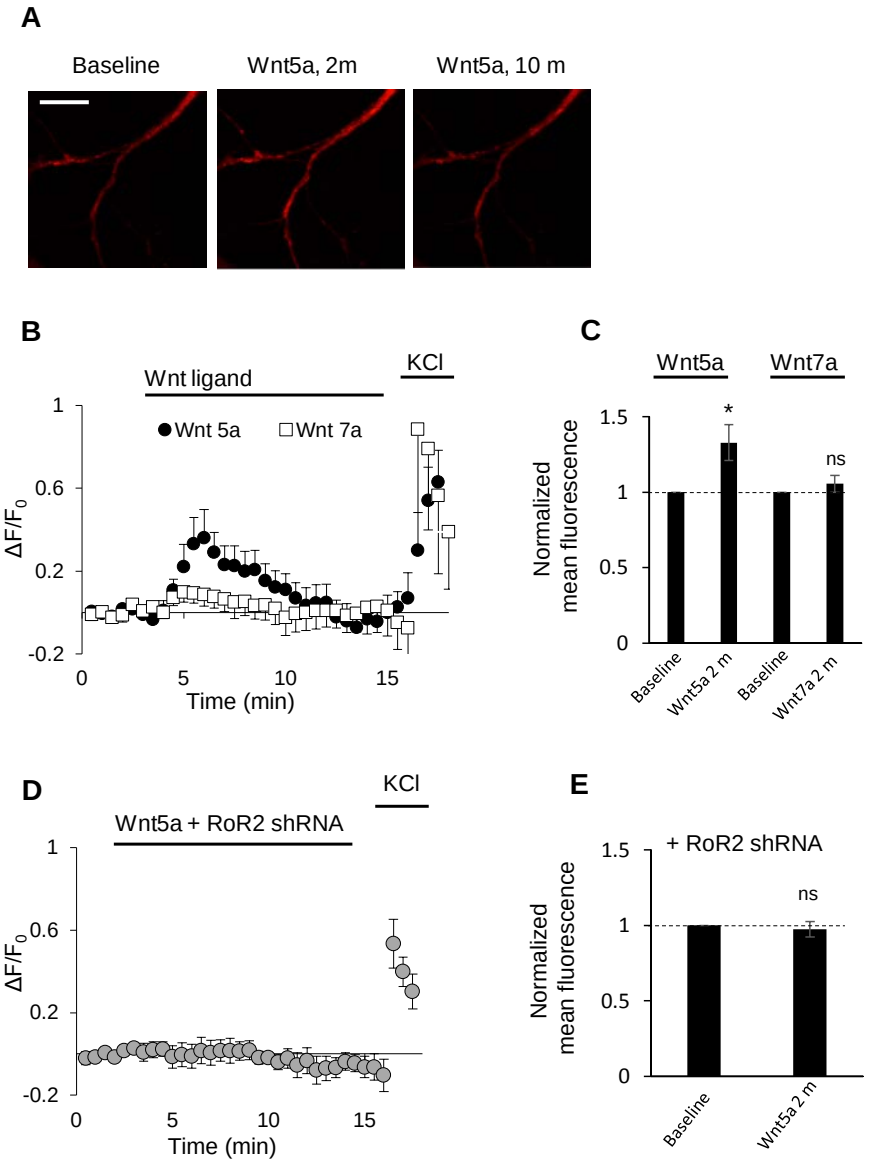

Figure 2.1 Wnt5a mobilizes intracellular Ca^{2+}. A. Dendrites of a dissociated CA1 neuron loaded with 3 μM Asante Calcium Red (ACR) at baseline, 2 and 10 minutes after adding Wnt5a to the bath. Scale bar =10 μm. **B.** Change in ACR fluorescence normalized to baseline. Either Wnt5a (black circles; n=15) or Wnt7a (white squares; n=8) was added to the bath after a 3-minute of baseline. ACSF containing 50 mM KCl was added to the bath as a positive control. **C.** Quantification of the normalized mean fluorescence signal at baseline and 2 minutes following either Wnt5a or Wnt7a to the bath. **D.** Change in ACR fluorescence from baseline as in B induced by Wnt5a in neurons expressing shRNA targeting the RoR2 receptor (n=10). **E.** Quantification of the normalized mean fluorescence signal at baseline and 2 minutes after adding Wnt5a to the bath in neurons transfected with an shRNA targeting RoR2. * $p < 0.05$.

Under these conditions, Wnt5a failed to elevate cytoplasmic Ca^{2+} (Figure 2.2 C and D). We concluded from these experiments that a combination of extracellular Ca^{2+} and Ca^{2+} from intracellular stores is necessary to initiate a full Wnt5a mediated Ca^{2+} response. This is consistent with previously shown mechanisms of calcium-induced calcium release (CICR) in excitable cells [90].

Further in agreement with the need for extracellular Ca^{2+} to initiate CICR from intracellular stores, blockade of (VGCC) L, N, P, and Q-type voltage gated Ca^{2+} channels with a cocktail containing nifedipine and ω-conotoxin MVIIC also blocked the increase in cytosolic Ca^{2+} initiated by Wnt5a (Figure 2.2 E and F). We tested next whether this Wnt/Ca^{2+} pathway also requires IP3 generation via phospholipase C (PLC), as it has been described for CICR involving Wnt5a signaling in zebrafish embryos [80]. To test this hypothesis, neurons were pre-incubated with PLC inhibitor U73122. As shown in Figure 2.2G and H, Wnt5a was still able to significantly elevate cytoplasmic calcium levels by 9 ± 3% ($p < 0.05$), though the response amplitude was much reduced compared with untreated neurons. Together, these experiments indicate that Wnt5a activates a mechanism leading to Ca^{2+} mobilization from stores requiring PLC activity, extracellular Ca^{2+}, and VGCCs to initiate the signal.

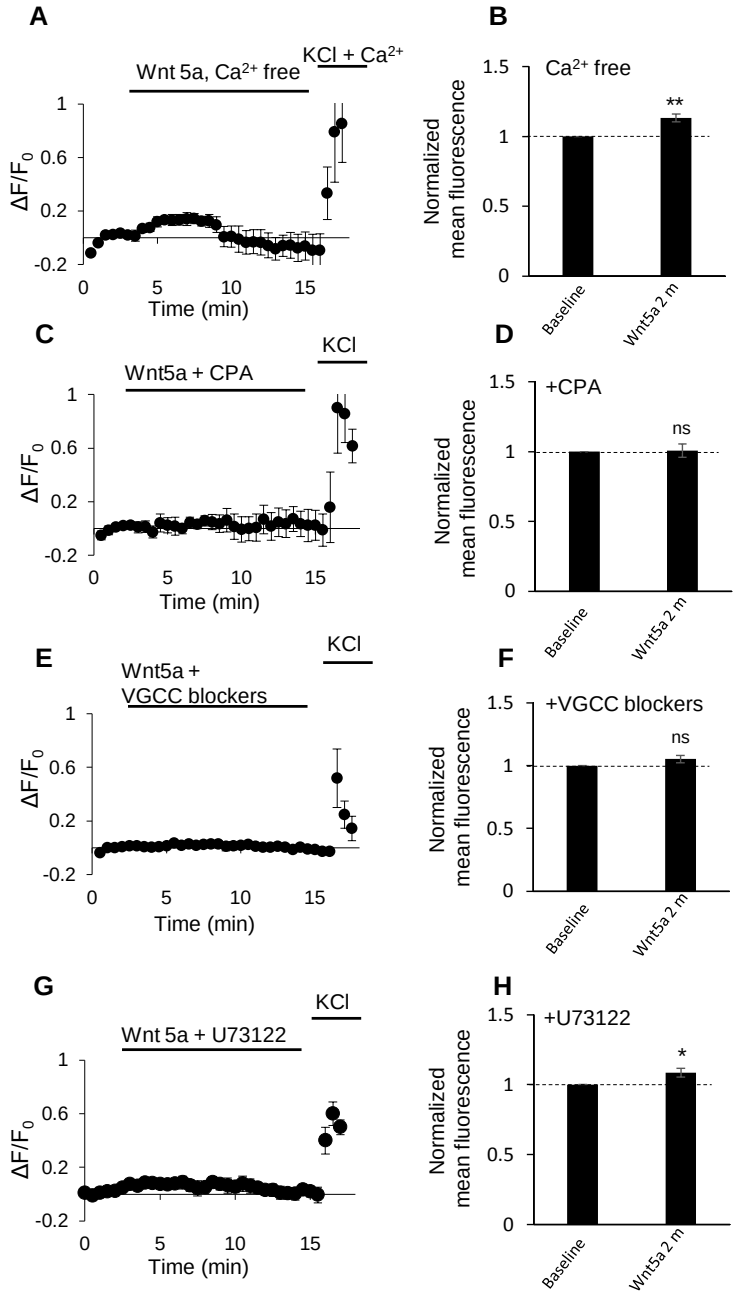

Figure 2.2 Wnt5a mobilizes intracellular Ca^{2+} from intracellular stores. Change in ACR fluorescence over time (left) and quantification of the mean fluorescence 2 min after Wnt5a addition to the bath, normalized to baseline (right) in neurons bathed in nominally Ca^{2+} free ACSF (n=8) (**A and B**), pretreated with 30 μM CPA (**C and D;** n=8), in the presence of 10 μM nifedipine and 1 μM ω-conotoxin MVIIC (**E and F**; n=6), or pretreated with 5μM PLC inhibitor, U73122 (**G and H**; n=8). * $p < 0.05$, ** $p < 0.01$.

We then tested whether this Wnt-mediated Ca^{2+} rise plays a role in Wnt5a's ability to potentiate NMDAR currents in hippocampal slices. As shown previously [64], Wnt5a significantly increased the amplitudes of pharmacologically isolated NMDAR currents recorded from hippocampal CA1 neurons 123 ± 38% compared to baseline over the course of an hour ($p < 0.01$, Figure 2.3A and E). This potentiation was reduced when slices were preincubated and bathed with CPA during the experiment to empty intracellular calcium stores (Figure 2.3B and E). To examine more carefully the role of voltage gated calcium channels in this cascade, we blocked the L-type calcium channel with nifedipine. We chose to focus on the L-type channel because of its well-documented role in postsynaptic calcium handling in hippocampus [53], and, because of its primarily postsynaptic function, we could include it in the bath for this electrophysiological paradigm without blocking glutamate release, as confirmed when nifedipine alone was added to the bath (not shown). This does not exclude a potential role for other VGCCs in this Wnt signaling cascade. When nifedipine was included in the bath, Wnt5a failed to potentiate NMDAR currents, instead inducing NMDAR rundown (Figure 2.3C and E). To examine the role of PLC in Wnt5a-mediated NMDAR potentiation, we pretreated and bathed neurons with U73122 during the experiment. This treatment also reduced NMDAR potentiation (Figure 2.3D and E).

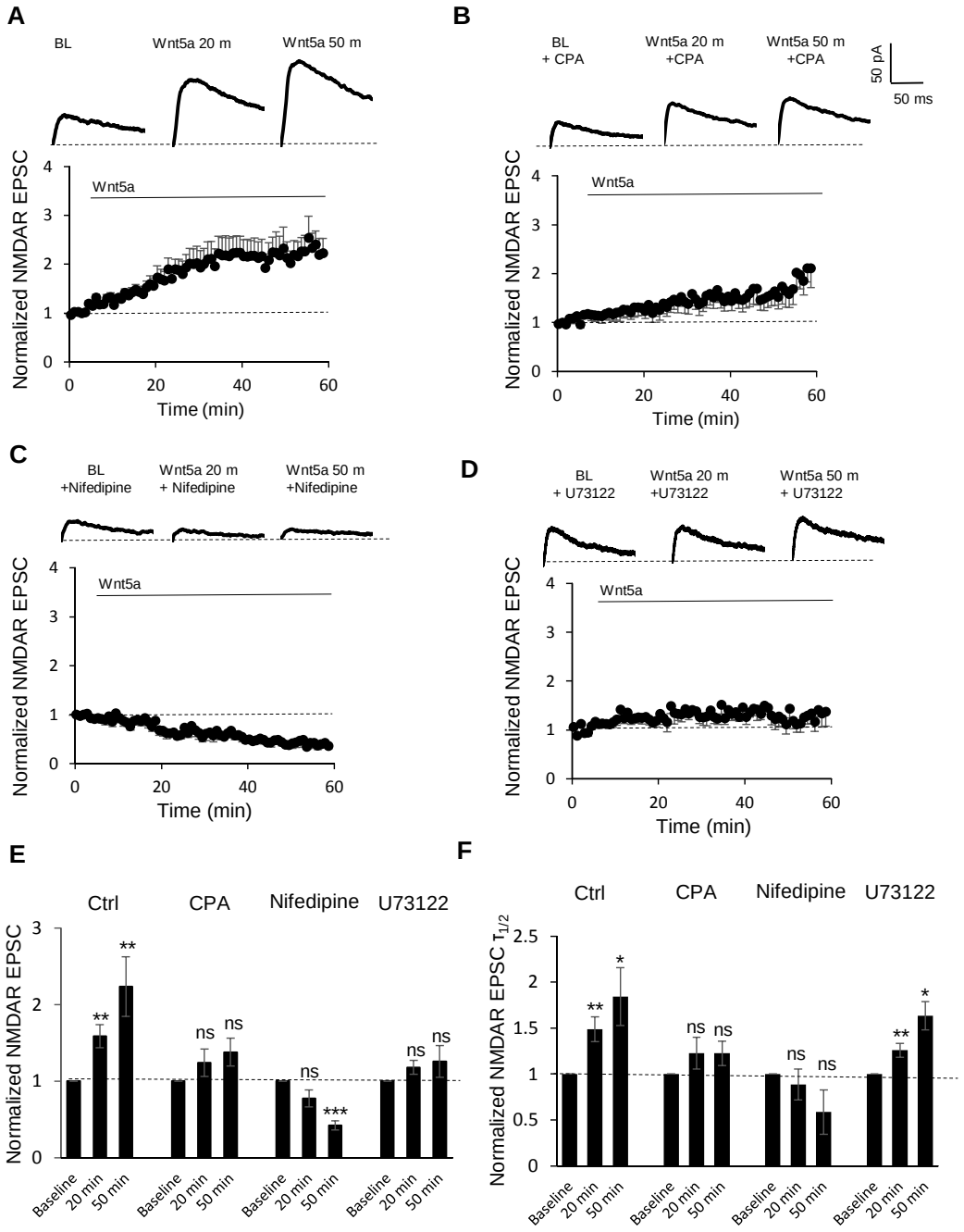

Figure 2.3 Intracellular Ca^{2+} release from stores is necessary for Wnt5a to upregulate NMDAR currents. **A.** Top, sample traces of isolated NMDAR-mediated EPSCs recorded at +40 mV during baseline, 20, and 50 minutes after bath application of Wnt5a from control neurons. Bottom, normalized peak amplitude of NMDAR-mediated EPSCs when Wnt5a was added to the bath (n=10). These experiments were performed with CA1 neurons in cultured hippocampal slices. **B.** Sample traces and normalized peak amplitude of NMDAR EPSCs as in A in neurons pretreated and bathed with 30 μM CPA during the experiment (n=9). **C.** Sample traces and normalized peak amplitudes of NMDAR EPSCS as in A in the presence of 10 μM nifedipine (n=9). **D.** Sample traces and normalized peak amplitude of NMDAR EPSCs as in A in neurons pretreated with 5μM U73122 (n=13). **E.**Quantification of NMDAR amplitudes at baseline, 20, and 50 minutes following Wnt5a treatment for the four conditions above. **F.** EPSC time to half decay for currents evoked at baseline, 20 and 50 minutes following Wnt5a treatment for the four conditions. * $p < 0.05$, ** $p < 0.01$, *** $p < 0.0005$

Consistent with our previous work, 50 minutes Wnt5a treatment also significantly increased the decay time constant of the NMDAR EPSC by 84 ± 31 % ($p < 0.05$ compared to baseline, Figure 2.3F, [64]). This increase, indicative of heightened representation of NMDARs containing the GluN2B subunit, was blocked by CPA incubation, and treatment with nifedipine. Wnt5a was able to significantly increase the time constant of neurons from slices pretreated with U73122 by 63 ± 15% (p <0.05), though not to the same degree as untreated slices.

Thus, Wnt5a can upregulate NMDAR currents through a mechanism that likely involves release of calcium from internal stores.

2.3.2 Wnt5a depolarizes CA1 neurons.

The role of VGCCs, particularly the L-type calcium channel, in the Wnt5a-mediated calcium elevation and NMDAR EPSC potentiation inspires the intriguing question of how Wnt5a engages these channels. We sought to see if Wnt5a depolarizes CA1 neurons. Electrophysiological recordings from hippocampal CA1 neurons in current clamp show that Wnt5a addition to the perfusion depolarizes neurons within 2 minutes (Figure 2.4A and B). This depolarization continues for the next 20 minutes, leading to a 5.9 ± 1.1 mV depolarization as measured in the soma of neurons. Wnt5a depolarized neurons significantly more than Wnt7a, which depolarized neurons 1.2 ± 0.5 mV, and control conditioned medium containing no Wnt ligand, 1.3 ± 0.9 mV ($p < 0.05$, ANOVA and Tukey's multiple comparison test, Figure 2.4B and D). This indicates that this depolarization is specific to the non-canonical Wnt5a signaling pathway. Blocking L-type calcium channels with nifedipine, or intracellular perfusion of BAPTA via the recording pipette did not prevent Wnt5a-induced depolarization, indicating that Ca^{2+} is not necessary for Wnt5a-induced depolarization, and that membrane depolarization precedes intracellular Ca^{2+} elevation in this signaling cascade (Figure 2.4C and D). However, the PLC inhibitor U73122 significantly reduced

Wnt5a-mediated depolarization to 2.2 ± 0.7 mV, suggesting activation of a metabotropic pathway involving cleavage of phosphatidylinositol to depolarize neurons ($p < 0.05$, ANOVA and Tukey's multiple comparison test, Figure 2.4C and D). Depolarization induced by Wnt5a pushed the resting membrane potential of neurons closer to threshold, such that CA1 pyramidal neurons fired more action potentials in response to current injections in the presence of Wnt5a. Wnt7a, as expected, did not cause an increase in the firing rate (Figure 2.4E-H). In tandem with the observed depolarization, this increase in firing frequency was seen within minutes of Wnt5a bath application and reached a maximum 20-30 minutes after bath application of Wnt5a (Figure 2.4H).

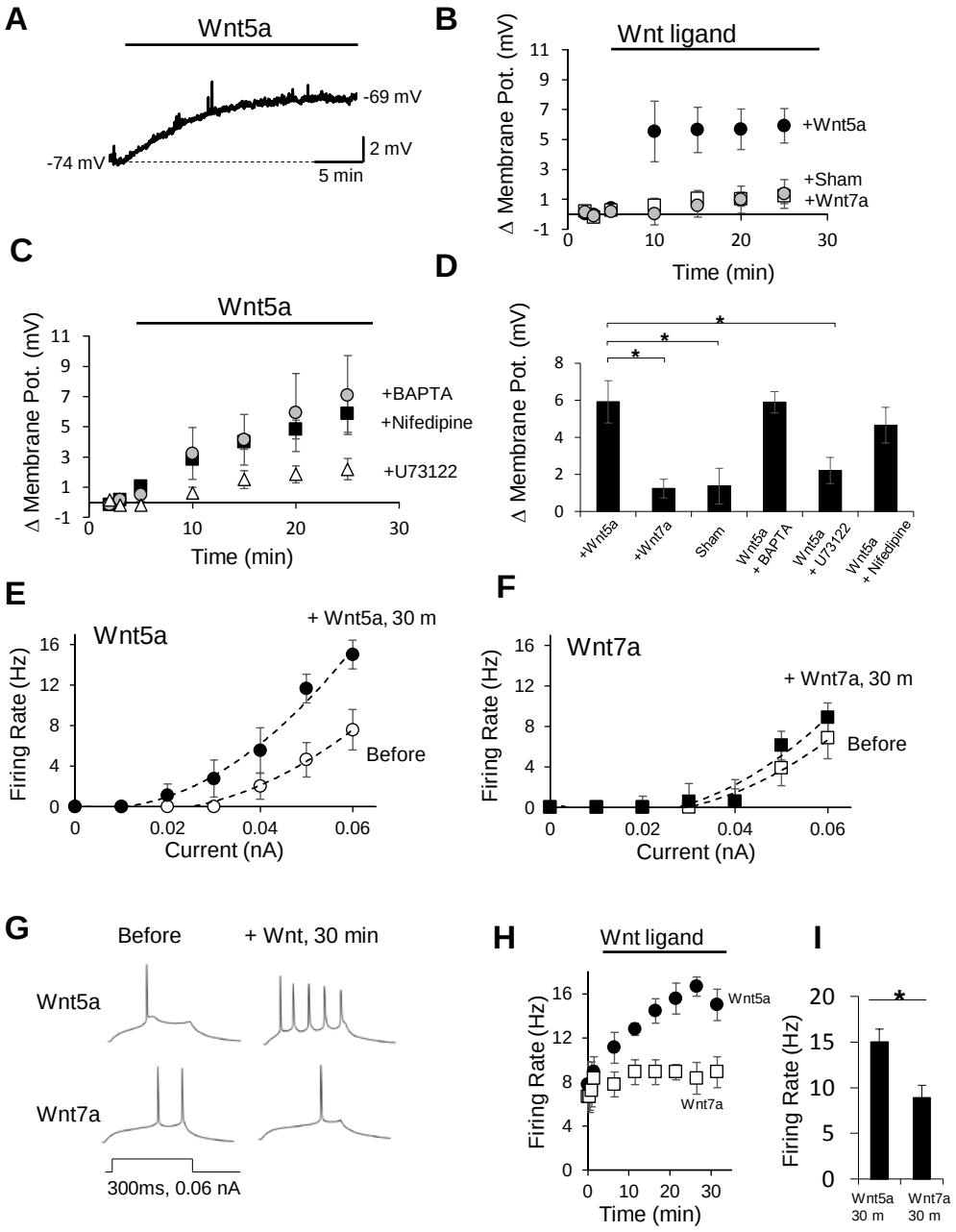

Figure 2.4 Wnt5a depolarizes CA1 neurons. A. Sample trace of resting membrane potential of a CA1 neuron in cultured hippocampal slice before and during bath application of Wnt5a. **B.** Average change in resting membrane potential over the course of 20 min. after bath application of Wnt5a (n=18), Wnt7a (n=9), or control conditioned media containing no Wnt ligand (n=11) as indicated. **C.** Average change in resting membrane potential over the course of 20 min. during bath application of Wnt5a to neurons recorded with 10 mM BAPTA in the patch pipette (grey circles; n=11), in the presence of 10 μM nifedipine (black squares; n=8), or pretreated with 5μM U73122 (white triangles; n=16). **D.** Absolute change in resting membrane potential after 20 min. bath application of Wnt5a for neurons treated as indicated. **E-F.** Input-output function for neurons before and 20 min after bath application of Wnt5a (E; n=6) or Wnt7a (F; n=6). Current steps were 300 ms. **G.** Sample traces of voltage response to a 0.06 nA, 300 ms, current injection before and during treatment with either Wnt5a (top) or Wnt7a (bottom). **H.** Frequency of action potentials per 300 ms, 0.06 nA current injection over the course of 20 min. during treatment with either Wnt5a (black circles; n=6) or Wnt7a (white squares; n=6). **I.** Quantification of firing frequency after treatment with either ligand. * $p < 0.05$

2.3.3. Wnt5a decreases current through K^+ channels, but does not affect resting ionic conductances or I_h.

To further understand how Wnt5a depolarizes neurons, we tested the effect of Wnt ligands on known contributors to the resting membrane potential. Wnt5a had no effect on resting leak currents as measured at the soma (Figure 2.5A). We also studied the effect of Wnt5a on I_h, a depolarizing, non-inactivating current mediated by hyperpolarization-activated cyclic nucleotide-gated ion channels (HCN), which stabilizes the membrane potential. We predicted that Wnt5a would decrease I_h if HCN were involved in this signaling cascade [91]. However, we saw no change in I_h upon Wnt5a addition (Figure 2.5B).

Wnt5a significantly reduced the steady-state current through high-voltage activated K^+ channels to 77 ± 3% of baseline values ($p < 0.0005$, Figure 2.5C, E, and F). Wnt7a also significantly reduced the potassium current to 86 ± 2.2% ($p < 0.005$, Figure 2.4D and E), though the reduction by Wn5a was significantly greater (unpaired t-test, $p < 0.05$). This reduction in high-voltage activated K^+ currents provides a mechanism by which Wnt5a could depolarize the membrane and initiate the Ca^{2+} signaling cascade. Inhibition of PLC with U73122 prevented the Wnt5a-induced reduction in these K+ currents (Figure 2.5G-I), indicating that activation of PLC is upstream of membrane depolarization and increase in cytosolic Ca^{2+}.

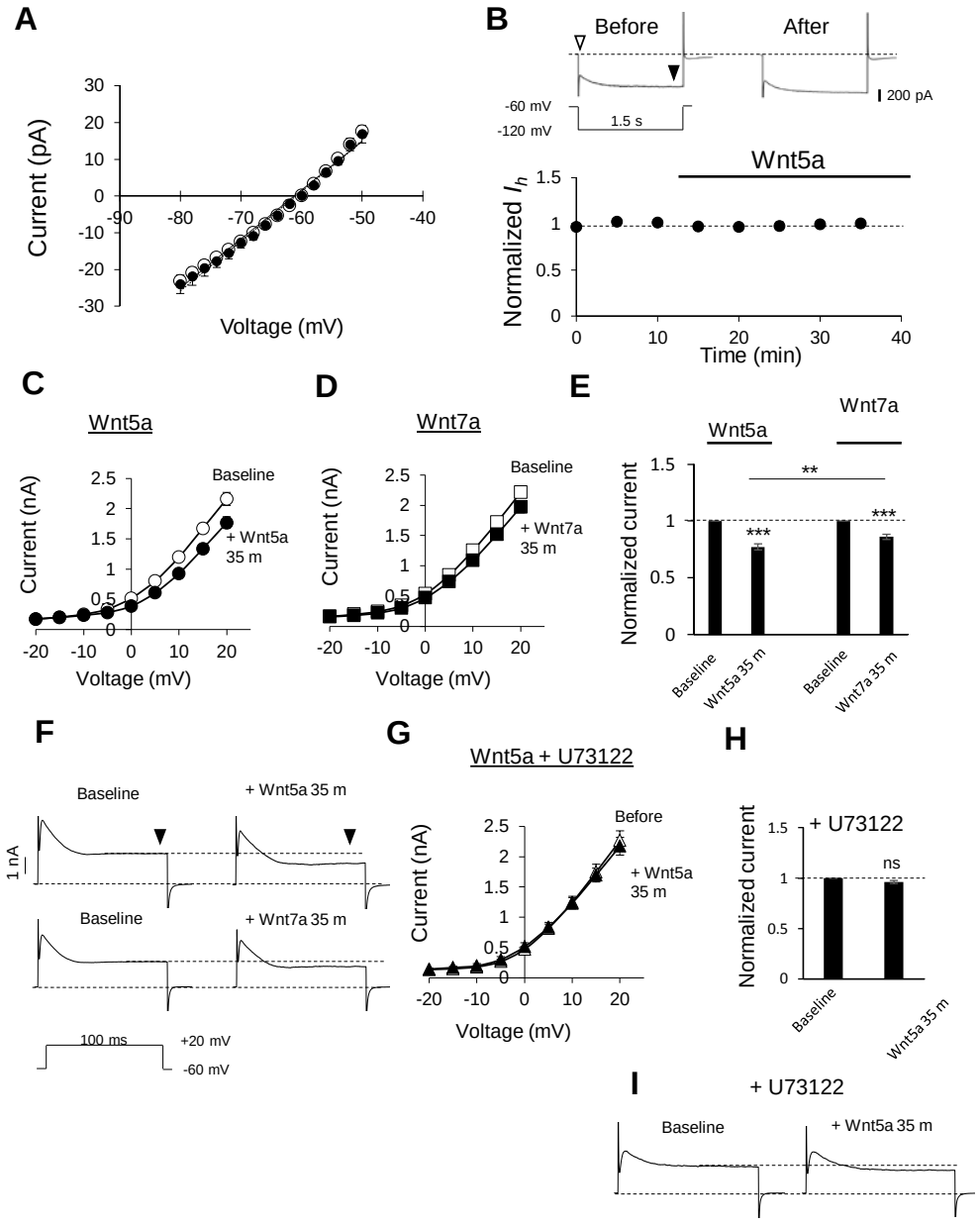

Figure 2.5 Wnt5a decreases current through high voltage activated K^+ channels, but does not affect resting conductance or I_h. A. Current-voltage relationship for leak currents evoked by 100 ms, 2 mV steps in the presence of 1 μM TTX to block voltage-gated sodium channels and 30 μM zd7288 to block I_h (n=6). **B.** Top, sample traces of I_h evoked by a hyperpolarizing voltage step to -120 mV before and after 30 min treatment with Wnt5a. I_h was measured by subtracting the instantaneous current (white arrow head) from the steady state current (black arrow head). Bottom, population data for normalized I_h before and after bath application of Wnt5a. **C-D.** Current-voltage relationship for K^+ currents acquired in the presence of 2 μM NBQX and 1 μM TTX before and 35 min after bath application of Wnt5a (C; n=7) or Wnt7a (D; n=6). **E.** Quantification of the reduction in K^+ currents induced by Wnt5a and Wnt7a following 35 min of treatment. **F.** Example traces of potassium currents evoked by a 100 ms step to +20 mV before and after 35 minutes of treatment with either Wnt5a (top) or Wnt7a (bottom). Steady-state current was measured at a window indicated by arrow-heads **G.** Current-voltage relationship for K^+ currents acquired in the presence of 2 μM NBQX, 1 μM TTX, and 5 μM PLC inhibitor U73122 before and 35 min after bath application of Wnt5a (n=9). Neurons were also pretreated with 5 μM U73122 at least 30 minutes before the experiment. **H.** Quantification of reduction in K^+ currents induced by Wnt5a in the presence of U73122. **I.** Example traces of K^+ currents as in E before and 35 min after Wnt5a treatment in the presence of U73122. ** $p < 0.01$, *** $p < 0.001$

2.3.4. Wnt5a promotes trafficking of GluN2B-containing NMDARs into synapses.

Wnt5a increases the amplitude of NMDAR-mediated EPSCs, the decay time constant of EPSCs, and the sensitivity of currents to the GluN2B specific antagonist ifenprodil, indicating an increase in synaptic NMDARs containing the GluN2B subunit [64]. We therefore asked if Wnt5a increased NMDAR EPSC amplitudes by promoting the trafficking of GluN2B-containing receptors to the surface.

To monitor surface expression of GluN2B-containing NMDARs, we tagged GluN2B subunits with pH-sensitive green fluorescent protein, super-ecliptic phluorin (SEP) [92] and transiently transfected this construct into dissociated hippocampal neurons. This construct will fluoresce only when exposed to the neutral extracellular space. Surface expression of NMDARs could then be monitored as the mean fluorescence for a dendritic ROI. At the end of each experiment, an impermeant low pH buffer (pH = 5.5) was added to the bath to quench surface fluorescence and confirm the measuring of surface fluoresce, not intracellular background. Cells were used for analysis only if the acid condition dropped fluorescence levels below baseline (not shown).

Wnt5a addition to the bath significantly increased the surface expression of GluN2B-containing NMDARs on primary and secondary dendrites by 20 ± 9% ($p < 0.05$, Figure 2.6A-C). In contrast, canonical Wnt ligand Wnt7a or control medium slightly reduced the surface expression of GluN2B-containing NMDARs, which may in part be due to photobleaching (Figure 2.6B and C). Knockdown of RoR2 in neurons eliminated the Wnt5a effect on NMDAR trafficking, confirming the specificity of the Wnt5a effect and the need of RoR2 for neuronal Wnt signaling [65] (Figure 2.6D and E). Pretreatment of neurons with CPA to empty internal Ca^{2+} stores (Figure

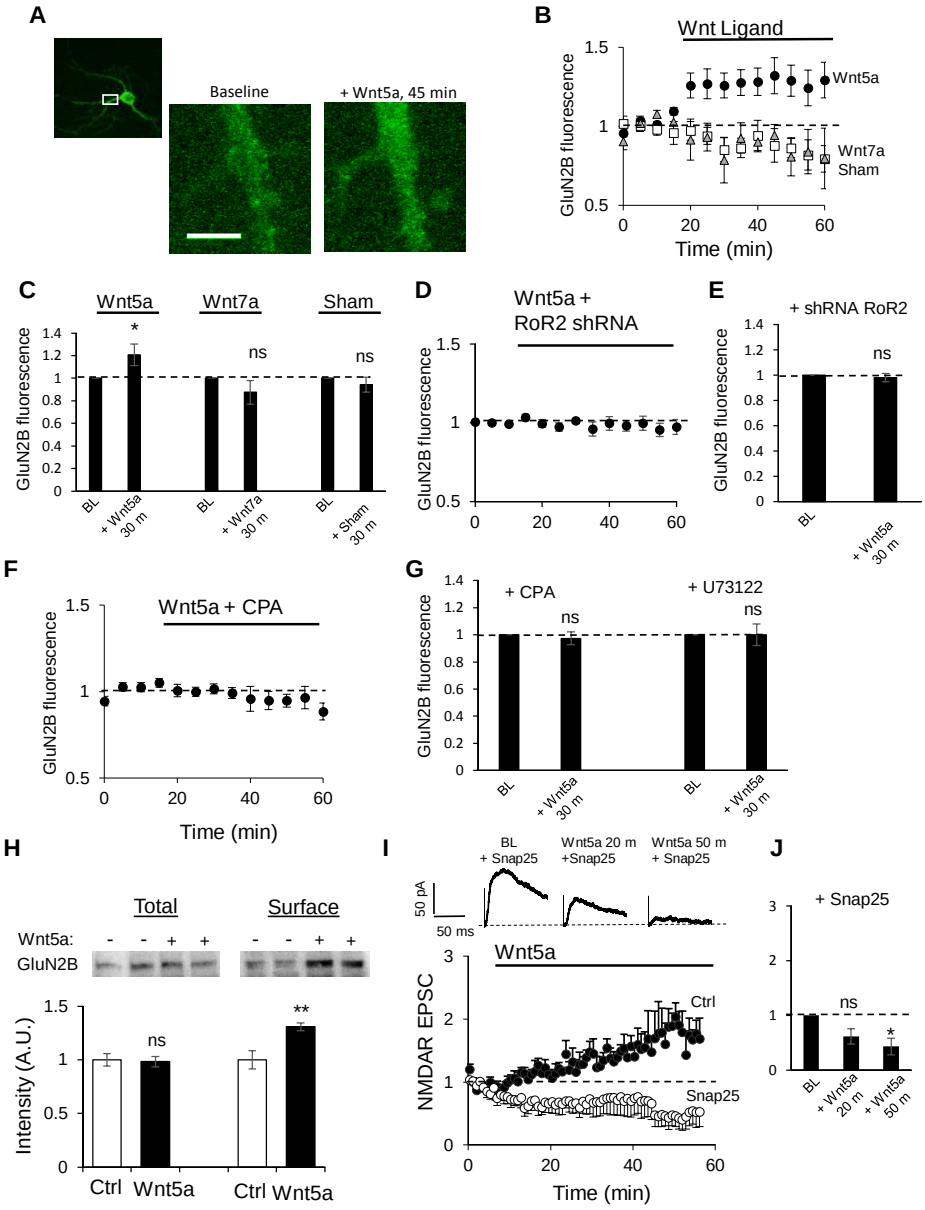

Figure 2.6 Wnt5a promotes trafficking of GluN2B-containing NMDARs. A. Dendrites of a dissociated hippocampal neuron transfected with SEP-tagged GluN2B at baseline and 45 minutes after adding Wnt5a to the bath. Inset: whole dissociated hippocampal neuron transfected with SEP-tagged GluN2B. Scale bar = 10 µm. **B.** Normalized surface fluorescence intensity in dendrites of dissociated hippocampal neurons expressing SEP-tagged GluN2B receptors before and after bath application of Wnt5a (black circles; n=8), Wnt7a (white squares; n=5), or control conditioned medium (grey triangles; n=3).**C.** Quantification of Wnt5a-induced change in mean fluorescence. **D.** Surface expression of GluN2B (as in B) in neurons expressing shRNA targeting the RoR2 receptor before and during treatment with Wnt5a (n=5). **E.** Quantification of Wnt5a induced changes in surface fluorescence in RoR2 knockout neurons. **F.** Surface expression of GluN2B (as in B) in neurons pretreated and bathed with 30 µM CPA before and during bath application of Wnt5a (n=5). **G.** Quantification of mean surface fluorescence change induced by Wnt5a of SEP-tagged GluN2B transfected neurons treated with CPA or U73122. **H.** Biotinylation of surface endogenous GluN2B. Top, sample immunoblot of total and surface GluN2B from control neurons or neurons treated for 1 hr with Wnt5a. Bottom, quantification of immunoblots intensity (n=8). **I.** Top, sample NMDAR EPSCs evoked at baseline, 20, and 50 min following Wnt5a addition to the bath with 10 µM SNAP25 in the patch pipette. Bottom, normalized peak amplitude of isolated NMDAR-mediated EPSCs recorded at +40 mV from control CA1 neurons (black circles; n=5) and neurons recorded with 10 µM Snap25 peptide in the patching pipette (white circles; n=5). This experiment was performed in cultured hippocampal slices. **J.** Quantification of the effects of Wnt5a on NMDAR EPSCS in the presence of SNAP25 in the patch pipette. * $p < 0.05$, ** $p < 0.01$.

2.6F and G) and treatment of neurons with U73122 (Figure 2.6G) abolished the Wnt5a mediated SEP-GluN2B surface increase.

We further confirmed the increase in surface expression of GluN2B by quantifying endogenous surface GluN2B in neuronal cultures using a biotinylation assay. Dissociated hippocampal neurons were treated for 1 hour with Wnt5a and surface proteins were biotinylated, immunoprecipitated, separated in SDS-PAGE, and immunoblotted using an anti-GluN2B antibody. As shown in Figure 2.6H, Wnt5a increased the amount of surface GluN2B 30 ± 4% ($p < 0.01$) without affecting the total amount of GluN2B. These data further corroborate that the Wnt5a/Ca^{2+} signaling pathway upregulates surface expression of NMDARs.

Insertion of glutamate receptors into the cell surface is a process mediated by SNARE proteins [22, 93]. To electrophysiologically test the role of receptor trafficking in Wnt5a-mediated NMDAR potentiation, we blocked receptor insertion using a SNAP25 peptide (aa 182-192, MEKADANKTRI) in the patch pipette. This peptide disrupts the interaction of endogenous SNAP25 with its binding partners, syntaxin-1 and VAMP2 [22]. Isolated NMDAR EPSCs were monitored in hippocampal CA3-CA1 synapses before and after bath application of Wnt5a. As described before, Wnt5a induced a potentiation of NMDAR-mediated currents (Figure 2.6I and J). Disruption of the exocytotic machinery with SNAP25 peptide blocked potentiation of NMDAR EPSCs induced by Wnt5a, and instead induced a slow rundown (Figure 2.6I). Together these experiments indicate that Wnt5a triggers a neuronal Wnt/Ca^{2+} signaling cascade that increases NMDAR trafficking, and hence measured NMDAR currents.

2.4 Discussion

The role and mechanisms of Wnt signaling have been extensively studied in embryonic development. Comparatively, its role in the postnatal brain is still elusive. Gene expression of Wnt

signaling components occurs in the postnatal brain lasting into adulthood, suggesting Wnt signaling has a role beyond early stages of development. It has been proposed that noncanonical Wnt ligands can regulate brain function via regulation of synaptic NMDARs [64].

Here we describe a neuronal noncanonical Wnt signaling cascade that mobilizes intracellular Ca^{2+} to upregulate trafficking of NMDARs with the final consequence of enhancing synaptic NMDAR-mediated currents. Figure 2.7 describes the signaling cascade: The non-canonical Wnt5a ligand binds to the RoR2 receptor, a tyrosine kinase-like orphan receptor recently identified as a receptor for noncanonical Wnt ligands [94, 95], and a mediator of Wnt5a-induced NMDAR potentiation [65]. Wnt5a binding RoR2 activates PLC, leading to a decrease in potassium currents, a subsequent rise in the membrane potential towards threshold, and VGCC-dependent mobilization of Ca^{2+} from intracellular stores. This ultimately increases the trafficking of NMDARs into synapses.

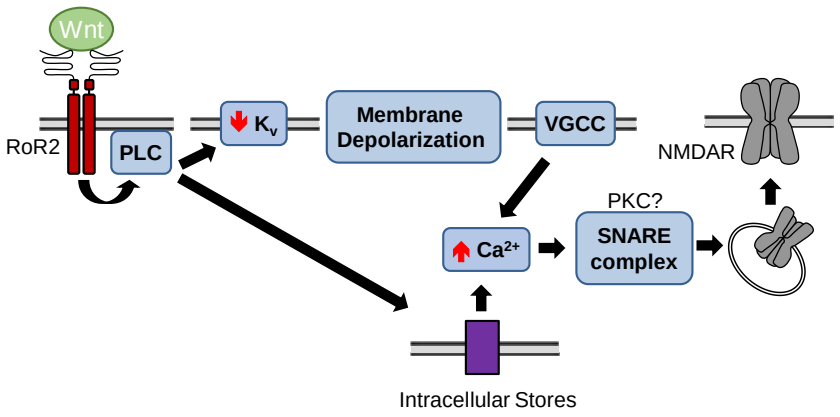

Figure 2.7 Model of Wnt/Ca^{2+} signaling in neurons. Wnt5a binds to RoR2 to activate PLC, leading to a decrease in potassium currents, a subsequent depolarization, and VGCC-dependent mobilization of Ca^{2+} from intracellular stores. This ultimately increases the trafficking of NMDARs into synapses.

Wnt ligands used here as representative canonical and non-canonical Wnt ligands, Wnt7a and Wnt5a respectively, are expressed in several regions of the brain of rodents. In particular, Wnt5a expressing cells are scattered through the neocortex and hippocampal formation in pyramidal and other layers in young adults [96], its mRNA is detected in the mature hippocampus [97], and the Wnt5a protein is detected in the conditioned medium of primary cultured astrocytes and neurons [84, 98]. This indicates Wnt5a may play a role regulating glutamatergic synaptic transmission. It would be important in the future to determine how the secretion of neuronal Wnt ligands is regulated and whether it is affected by synaptic activity.

The depolarization of the membrane observed upon Wnt5a addition to the bath may be orchestrated by the closing of the KCNQ channels. These channels mitigate the *m* current, and are up regulated by phosphatidylinositols, which leads to the intriguing possibility that cleavage of PIP2 via PLC activation results in PIP2 depletion and channel closure [99]. The fact that Wnt5a decreases the steady-state current through potassium channels in a PLC dependent manner is supportive of this mechanism. The fact that we see no change in the currents at rest might be attributable to a space-clamp issue of doing these recordings in the soma, while the change in input resistance further away could be much greater.

Wnt5a depolarized neurons by roughly 6 mV, though again, if measured in distal dendrites, this change in membrane potential could be greater. Our data suggest that this depolarization is sufficient to engage VGCC and initiate a CICR response. Depolarization by local synaptic activity could also be required to summate with the Wnt5a-induced depolarization in order to gate VGCCs. This could represent a mechanism to upregulate NMDARs only on those dendrites where some synaptic activity exists.

The increase in intracellular Ca^{2+} triggered by noncanonical Wnt5a is slow and depends on the activation of PLC and VGCC, suggesting that the time course of the Ca^{2+} signal is not adequate to cause potentiation of AMPAR-mediated responses, which requires short and fast Ca^{2+} transients, as in long-term potentiation paradigms [11]. This explains the observed specificity of noncanonical Wnt to potentiate NMDARs but not AMPARs [64].

We also show that surface expression of NMDARs is increased by Wnt5a in a manner dependent of SNARE proteins. PKC activity is also necessary for Wnt5a-induced potentiation of NMDAR-currents, suggesting that SNAP25 could be a target of PKC activated by Wnt5a [64, 65]. While the increase in surface NMDARs seems modest (~30%) compared to the increase in synaptic NMDAR-mediated EPSCs (2-3 fold), this apparent discrepancy is because surface expression is measured globally in dendrites while currents are measured only at synapses. Thus, a global increase in surface GluN2B-containing receptors would increase lateral diffusion of NMDARs into synapses [100]. The depolarization, together with larger synaptic NMDAR currents mediated by the GluN2B subunit, will increase subsequent synaptic plasticity [24], giving Wnt signaling a key role in the regulation of brain function.

Our study describes a novel Wnt signaling cascade present in mature neurons that depolarizes cells and increases trafficking of NMDARs into synapses [64, 65]. This provides a cellular mechanism to explain how Wnt5a upregulates NMDA-mediated synaptic currents. Due to the importance of NMDARs in synaptogenesis, synaptic plasticity, and neuropathologies, regulation of Wnts may be critical for brain function beyond embryonic development. In addition, this novel Wnt/Ca^{2+} signaling mechanism could contribute to the proper Ca^{2+} handling that is necessary for proper synaptic physiology and that is disrupted in neuropathologies. Future studies regarding the

regulation and secretion of Wnt ligands in the mature hippocampus may lead to effective treatments for neuropathologies where glutamatergic transmission is compromised.

CHAPTER 3

Dynamic lateral exchange of synaptic and extrasynaptic NMDARs

3.1 Introduction

The *N*-methyl-D-aspartate receptor (NMDAR) is an ionotropic glutamate receptor expressed throughout neocortex, permeable to calcium, and is fundamental for both synaptogenesis and experience-driven synaptic plasticity. Although historically NMDARs have been thought to be relatively stable components of synapses based on their tight association with scaffolding proteins [7, 101], more recent evidence elucidates that NMDARs are dynamic, making understanding the intracellular mechanisms that control their expression and function imperative [51].

Decreasing neuronal activity promotes NMDAR function at synapses in the hippocampus: pharmacological treatment of cultured hippocampal neurons with TTX increases NMDAR surface expression [57]. Consistently, preventing glutamate from binding NMDAR with APV treatment increases receptor localization to synapses [58]. APV also increases NMDAR phosphorylation states in a manner supportive of surface expression [102]. However, many of these pharmacological modifications have been studied over the course of hours or even days. Considering that synapses can change their characteristics within minutes, it is crucial to evaluate how activity might modify NMDAR representation within synapses on a shorter time scale. We have previously shown that a 15-minute period of silence following 0.1 Hz stimulation potentiates synaptic NMDAR currents [59], but the mechanisms behind this phenomenon are still unclear.

One aspect of NMDAR regulation that has not been well elucidated is lateral surface movement between extrasynaptic and synaptic compartments. On postsynaptic sites, NMDARs

are located both synaptically and extrasynaptically, and synaptic vs. extrasynaptic NMDARs are proposed to have different subunit compositions and functions via association with different signaling platforms [103, 104]. Whether there is exchange between synaptic and extrasynaptic receptor pools is unclear. Using the activity-dependent NMDAR inhibitor, MK-801, it has been demonstrated in autaptic hippocampal dissociated neuronal cultures that NMDARs can move laterally into synaptic regions [105]. Quantum receptor tracking further supports that NMDARs diffuse quite readily on the plasma membrane surface at a rate determined by subunit composition [100, 106]. However, this mobility has not been demonstrated in more intact systems such as hippocampal slices, and some evidence supports that in the more physiological paradigm, synaptic and extrasynaptic receptors are fixed, calling into question whether such mobility occurs *in vivo* [107]. In addition, it is also unclear what mechanisms, whether intracellularly or extracellularly, govern this lateral mobility.

In this report, we sought to re-investigate whether NMDARs move between synaptic and extrasynaptic compartments in hippocampal slices. We have found evidence supportive of NMDAR exchange, as responses can recover from synaptic block with MK-801. This recovery is activity-dependent, but calcium independent, and may be attributable to NMDARs containing the GluN2B subunit. Consistent with previous studies of activity-dependent NMDAR regulation, we also demonstrate that a period of silence following stimulation promotes this receptor movement into synapses. Such exchange might produce a mechanism by which synapses can rapidly change their threshold for plasticity. Considering the fundamental role of NMDARs in learning, and their implication in neuropathologies, it is of crucial importance to clarify if these receptors traffic laterally between compartments as a means of fine-tuning synaptic characteristics on a minute-by-minute basis.

3.2. Materials and methods

Hippocampal slices

Organotypic hippocampal slices (400 μm thick) were prepared according to standard procedures from postnatal day (P)6-9 male and female Sprague Dawley rats and maintained in culture for 3-8 days at 35°C. Animals were handled in accordance with University of Washington (Seattle, WA) institutional animal care and use committee guidelines.

Electrophysiology

For each experiment, the CA1 area of a hippocampal slice was isolated by making two cuts flanking the CA1 region, and then the slice was placed into the recording chamber containing modified ACSF (mACSF): (in mM) 10 Glucose, 2.5 KCl, 118 NaCl, 1 NaH2PO4, 2 CaCl2, 2 MgCl2, 26 NaHCO3, pH 7.4, constantly circulating and bubbled with 95% O2, 5% carbon dioxide. NMDAR mediated currents were recorded from CA1 neurons patched under visual guidance with glass pipettes (~2-4 MΩ) filled with a cesium based internal solution: (in mM) 115 CsMeSO4, 20 CsCl2, 10 Hepes, 2.5 MgCl2, 4 MgATP, 0.4 Na3GTP, 10 Na-phosphocreatine, 0.6 EGTA, pH 7.25. Currents were evoked by holding the cells at depolarized potentials below the NMDAR reversal potential (between -40 and -15 mV, average -30 mV) and stimulating the Schaffer collaterals with a bipolar cluster electrode (CE2C55, FHC) placed about 100 μm away from the cell of interest. To isolate NMDAR currents, NBQX (2μM) and picrotoxin (100μM) were also included in the bath. Temperature was kept between 22.8-23.0°C. Recordings were obtained with a MultiClamp 700B amplifier (Axon Instruments) and pClamp 10.1 software.

Statistics

Where appropriate, statistical significance was determined using a Student's standard t-test, with $p < 0.05$ considered statistically significant.

3.3. Results

3.3.1 NMDAR EPSCs are rapidly and bidirectionally modified by activity.

We have previously reported that a decrease in stimulation frequency can potentiate NMDAR currents, indicating that NMDARs within synapses can be rapidly regulated by changes in activity [59]. These results were obtained from neurons voltage clamped at +40 mV to activate NMDARs. We first repeated this experiment voltage clamping at hyperpolarized potentials (average, ~-30 mV), which is closer to physiological conditions. The holding potential and stimulation amplitude was adjusted for each cell to produce an EPSC of consistent size (~25-50 pA). Similar to what we found previously, reducing the stimulation frequency from 0.1 Hz to 0.05 Hz for 20 min resulted in a significant potentiation of NMDAR currents by 44 ± 12% when compared with baseline ($p < 0.05$, Figure 3.1A-C). Once 0.1 Hz stimulation was resumed, potentiated NMDAR EPSC response amplitudes began to decline back to baseline. In tandem, when stimulation frequency was increased from 0.1 Hz to 0.5 Hz, NMDAR EPSC amplitudes significantly declined to 87 ± 5% of baseline values ($p < 0.05$, Figure 3.1D-F). Completely stopping stimulation for only 5 minutes significantly increased NMDAR EPSC amplitudes over baseline by 18 ± 6% (Figure 3.1G-I, $p < 0.01$).

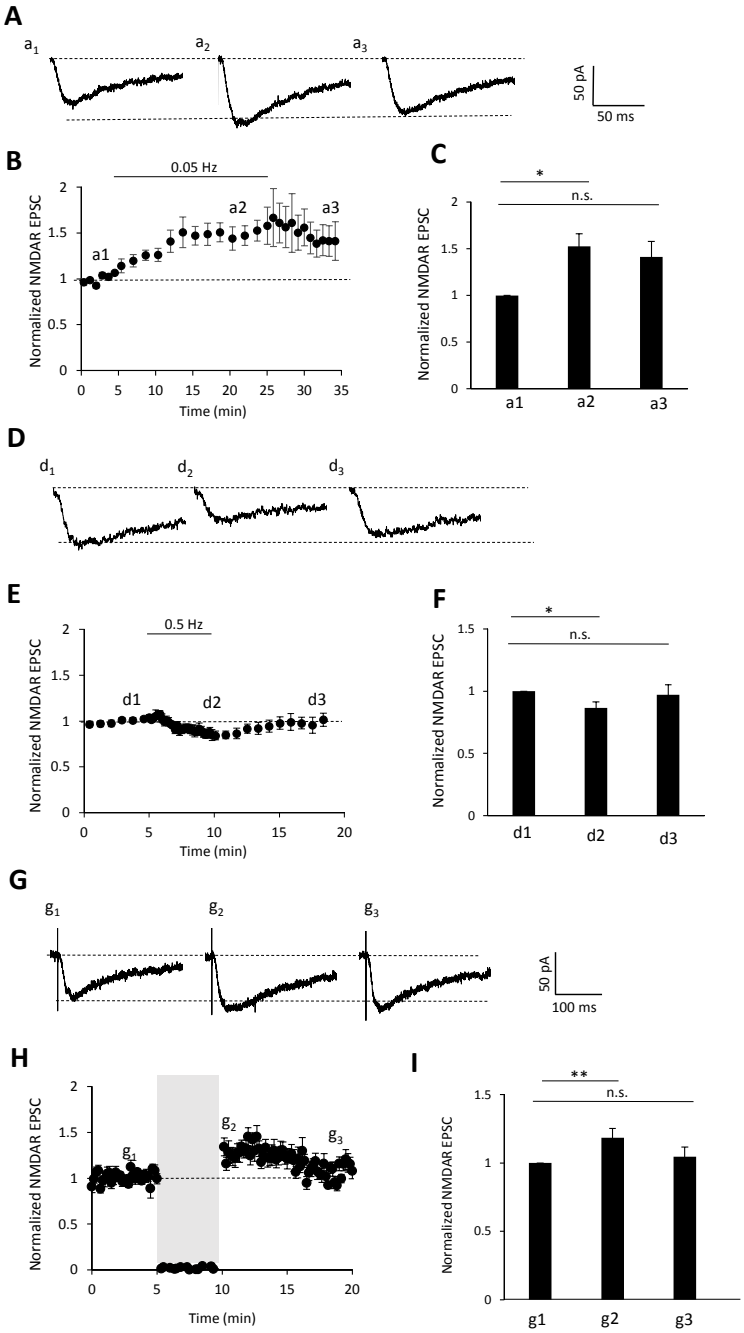

Figure 3.1 Activity bidirectionally regulates NMDAR currents. A. Example isolated NMDAR EPSC traces evoked from CA1 cells in hippocampal slices at baseline stimulation of 0.1 Hz (a1), after 20 minutes at 0.05 Hz stimulation (a2) and 10 minutes after 0.1 Hz stimulation was resumed (a3). **B.** Normalized average NMDAR peak amplitudes when the stimulation frequency was decreased (n = 4). Points here represent the average of five evoked currents. Here and in all figures, error bars represent the standard error of the mean. **C.** Quantification of changes in NMDAR amplitude at the times indicated. **D.** Example isolated NMDAR EPSC traces at baseline stimulation of 0.1 Hz (d1), after 5 minutes at 0.5 Hz stimulation (d2), and 10 minutes after 0.1 Hz stimulation was resumed (d3). **E.** Normalized average NMDAR peak amplitudes when stimulation frequency was briefly increased (n = 10). **F.** Quantification of changes in NMDAR amplitude at the times indicated. **G**. Example isolated NMDAR EPSCs evoked from CA1 cells in hippocampal slices at baseline (g1) after 5 minutes without stimulation (g2), and 10 min after resuming stimulation (g3). **H.** Average peak amplitude of NMDAR EPSCs normalized to baseline when stimulation was briefly turned off (n =11). Gray bar indicates a period where there was no stimulation. **I.** Quantification of changes in NMDAR EPSC amplitude at the times indicated. * $p < 0.05$, ** $p < 0.01$.

Similar to Figure 3.1B, resuming 0.1 Hz stimulation returned responses back to baseline over the course of 10 minutes. Together, these data suggest that NMDARs can be rapidly modified by changes in activity [59].

3.3.2 NMDAR potentiation is due to lateral movement of surface receptors.

The observation that NMDARs potentiate following a period of silence led us to investigate the underlying mechanism. Considering the five-minute, relatively short time scale, one possibility is that the potentiation is carried by surface extrasynaptic receptors diffusing laterally into synapses. To investigate whether receptors were mobile, we used the activity - dependent non-competitive NMDAR antagonist, MK-801, which will irreversibly block activated receptors within stimulated synapses. Should receptors be fixed within synapses, each stimulus iteration should decrease the NMDAR EPSC amplitude until all receptors are eliminated and responses reach zero. We recorded a baseline at 0.1 Hz, then turned off stimulation for 5 minutes, at which time 5, 10, or 40 μM MK-801 was washed into the bath. These concentrations are well above the IC50 of MK-801 [108, 109]. The 5 minutes of silence allowed adequate time for even dissemination of the MK-801 throughout the ACSF. When stimulation was resumed, NMDAR EPSCs rapidly declined as expected. However, responses did not reach zero over the ten-minute period, and instead flattened out at a non-zero value following 10 minutes of exposure (60 stimulus pulses) for all three concentrations of MK-801 (Figure 3.2A-D). Responses only reached zero upon co-application of the competitive NMDAR antagonist DL-APV to the bath (100 μM). This pattern of blockade matches what has been seen by others [110] and can be fit with a single order exponential decay function (Figure 3.2F).

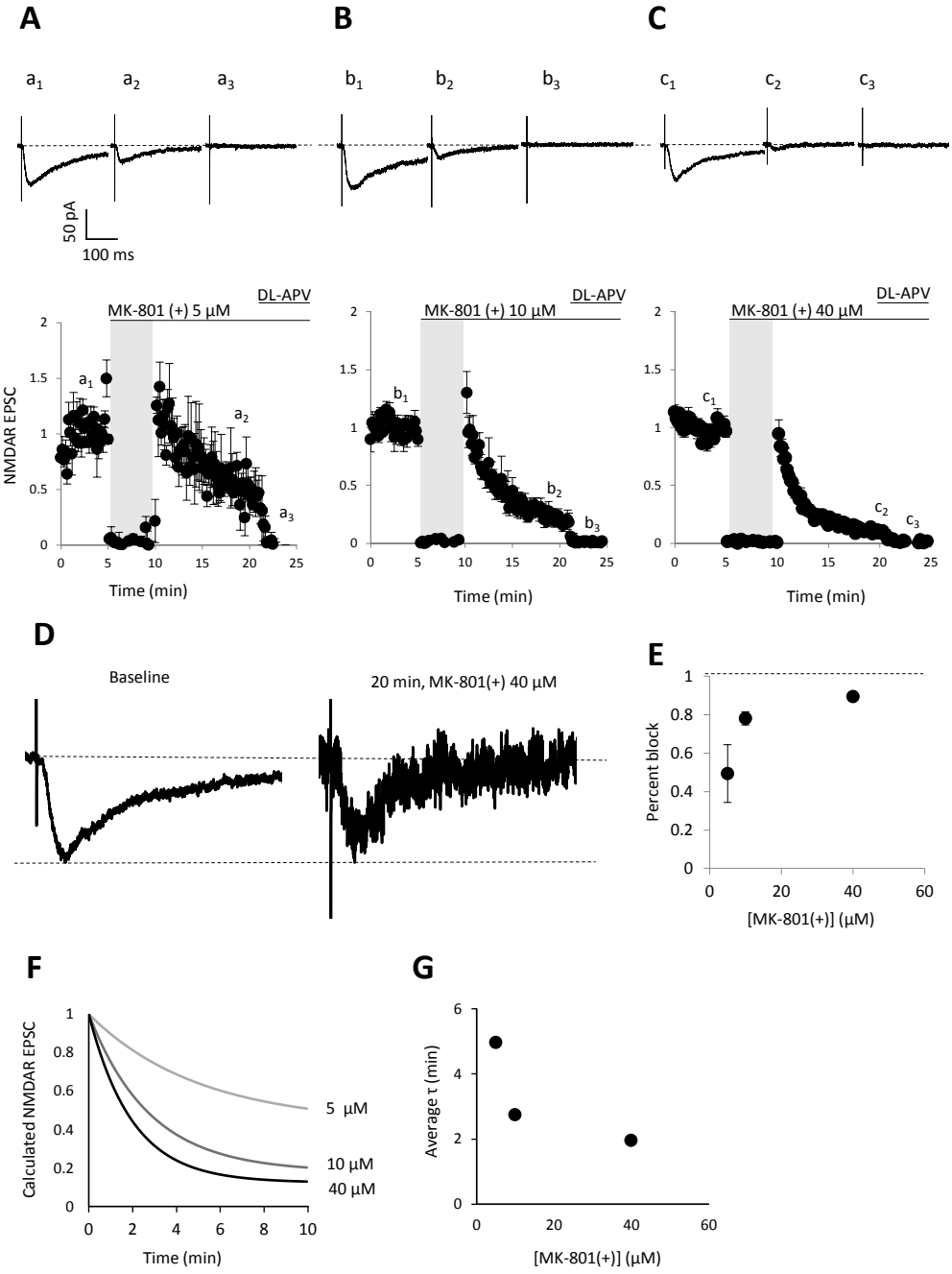

Figure 3.2 MK-801 and stimulation do not completely block synaptic NMDARs. A. (Top) Example NMDAR EPSCs obtained at baseline (a1), after ten minutes of 0.1 Hz stimulation in the presence of 5 μM MK-801 (a2), and in the presence of 100 μM DL-APV. (Bottom) Average NMDAR EPSC peak amplitude normalized to baseline (n =5). Gray bar indicates a period of no stimulation. **B.** Same as in A with 10 μM MK-801 (n =5). **C.** Same as in A with 40 μM Mk-801 (n=5). **D.** NMDAR EPSCs evoked at baseline and after ten minutes of 0.1 Hz stimulation in the presence of 40 μM MK-801 (same traces as in c1 and c2), normalized to the peak. **E.** Percent of baseline blocked by 60 stimulus pulses in the presence of MK-801 as a function of MK-801 concentration. **F.** Single exponential curves ($A = A_o * e^{(-t/tau)}$) fit to the average NMDAR EPSC blockade with 5, 10, or 40 μM MK-801 as indicated. **G.** Calculated time constant of the MK-801 blockade of NMDAR EPSCs as a function of MK-801 concentration.

Fits for all three concentrations reveal that the percentage of MK-801 blockade from baseline and the time constant of the blockade were dependent on MK-801 concentration in a non-linear manner (Figure 3.2E-G). The inability to reach complete blockade at this timescale and stimulation frequency suggests that synaptic receptors are not fixed, and potentially another population of receptors less susceptible to MK-801 prevents complete blockade.

If a decrease in activity potentiates synaptic NMDARs (Figure 3.1), and the potentiation is governed by receptors moving between extrasynaptic and synaptic compartments, (Figure 3.2), then a five-minute period of silence should result in at least a partial recovery from MK-801 and synaptic blockade. To ask if NMDAR EPSCs could recover from MK-801 blockade, stimulation was turned off following a 5-minute baseline, and MK-801 washed in as done in Figure 3.2. For these experiments, we consistently used 10 μM MK-801. Partial MK-801 blockade was induced by a total of 30 pulses delivered at 0.1 Hz. This rapidly reduced the amplitude of evoked NMDAR EPSCs to 45 ± 8% of baseline levels. Stimulation was turned off again for 5-minutes, during which MK-801 was washed out. Stimulation at 0.1 Hz was then resumed. NMDAR EPSC amplitudes recovered to on average 71 ± 9% of baseline *($p < 0.01$,* compared with the end of blockade) (Figure 3.3A-C). Over the course of 10 minutes, response amplitudes decreased back to values similar to the end of the MK-801 block (41 ± 9%), but did not decrease further. This decrease in the EPSC amplitude likely reflects the activity-dependent modulation of NMDAR EPSCs shown in Figure 3.1. The recovery was accompanied by significant increase in the EPSC time to half-decay (Figure 3.3C). There was no correlation between holding potential and percent recovery (not shown). Neither the percent blockade nor the percent recovery were dependent on baseline amplitude (blockade, $R^2 = 0.08$; recovery, $R^2 = 0.04$, Figure 3.3D).

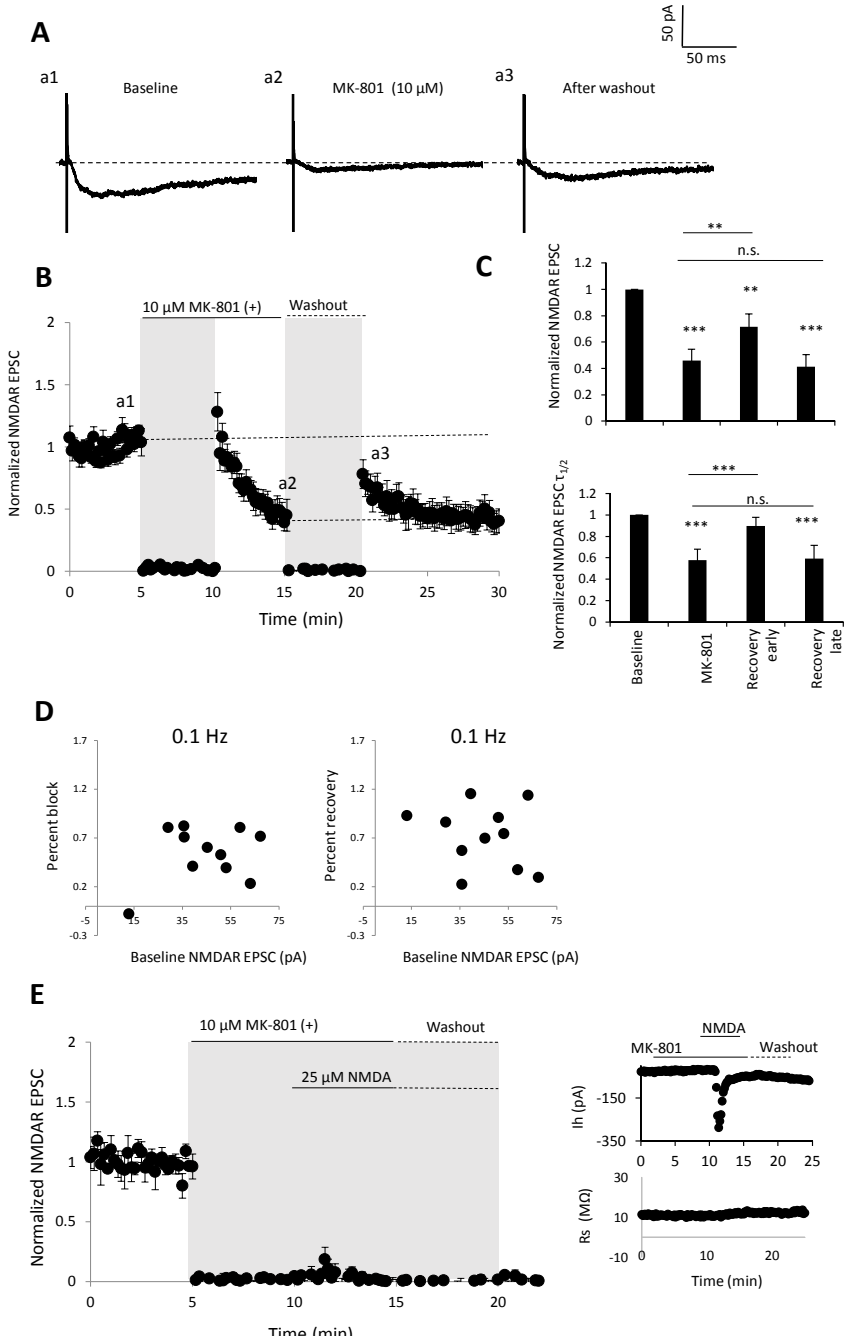

Figure 3.3 NMDAR EPSCs recover following synaptic blockade. A. Example NMDAR EPSCs obtained at baseline (a1), after 5 minutes of stimulation in the presence of 10 µM MK-801 (30 stimulus pulses) (a2) and immediately following washout (a3). **B.** Average NMDAR EPSC peak amplitude normalized to baseline during recovery experiment (n =11). Gray bar indicates periods of no stimulation. **C.** (Top) Quantification of NMDAR EPSC peak amplitude at the times indicated. (Bottom) Quantification of NMDAR EPSC time to half decay. **D.** Percent of baseline blocked as a function of the initial baseline EPSC amplitude (left), and percent of baseline recovered as a function of initial baseline EPSC amplitude (right) **E.** Left, average NMDAR EPSC peak amplitude during NMDA and MK-801 co-application experiment (n =5). Gray box indicates period of no stimulation. Right, the holding current (top) and series resistance (bottom) for the same example cell. *** $p < 0.01$, **** $p < 0.005$.*

To rule out whether this potentiation results from delivery of intracellular receptors to the surface, we co-applied the agonist NMDA (25 μM) with MK-801 to block all surface receptors, followed by a period of silence and washout as before. NMDA application resulted in a large depolarization as shown by the holding current, which quickly returned to baseline as MK-801 blocked open channels. Under these conditions, we observed no recovery when stimulation was resumed (Figure 3.3E).

These results support that NMDAR recovery from MK-801 block is mediated by receptors located on the surface that can move into synapses.

3.3.3. Exchange between synaptic and extrasynaptic NMDARs is rapid.

We also found a negative correlation between the percent of baseline MK-801 blocked and the percent of baseline recovered following washout (R^2 = 0.5, Figure 3.4A). This suggests that the receptors contributing to the recovery are influenced by the amount of induced blockade. In dissociated neurons, GluN2B-containing NMDARs move freely across dendrites, possibly continuously entering and leaving synaptic spaces [100]. It therefore follows that a constant level of receptor movement into or out of synapses might reach an equilibrium at a certain level of stimulation. To further examine this observation, we repeated the recovery experiment at 0.2 and 0.3 Hz stimulation frequency, which would increase the level of blockade by exposing receptors to an increased number of glutamate pulses and blockade by MK-801. We hypothesized it would concomitantly decrease the percent of baseline recovered. At 0.2 Hz (60 pulses), MK-801 blocked NMDAR EPSCs to 26 ± 7% of baseline values.

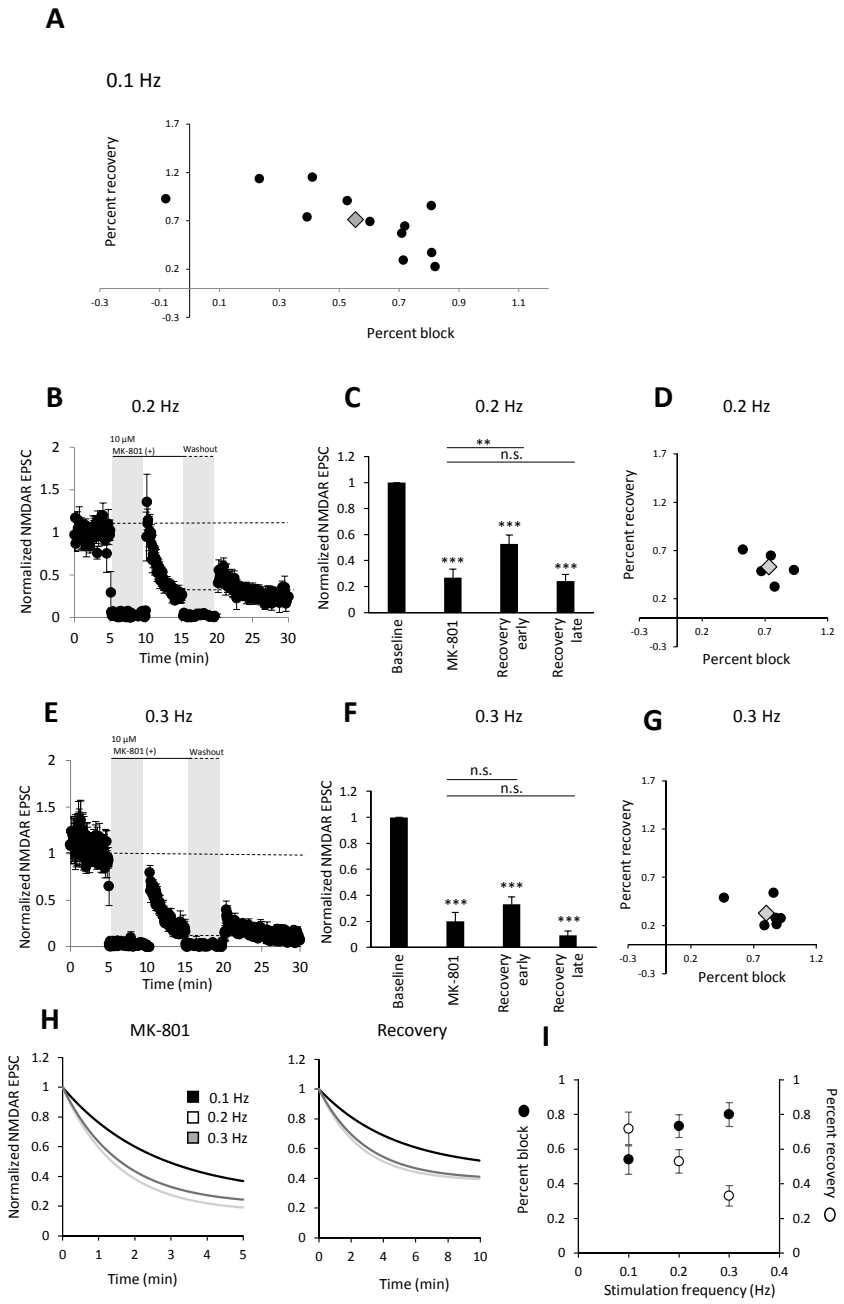

Figure 3.4 Increasing levels of block limits recovery. A. Percent of baseline recovered as a function of percent blockade. Each point (black circles) is one cell from Figure 3B. The gray diamond represents the average. **B.** Average NMDAR EPSC peak amplitude normalized to baseline, same experiment as in Figure 3B, but stimulation frequency was increased to 0.2 Hz (n = 5). **C.** Quantification of NMDAR EPSC amplitude at the times indicated. **D.** Percent of baseline recovered as a function of percent blockade for the 0.2 Hz experiment. **E.** Average NMDAR EPSC peak amplitude normalized to baseline when stimulation frequency was increased to 0.3 Hz (n =6). **F.** Quantification of NMDAR EPSC amplitude at the times indicated. **G.** Percent of baseline recovered as a function of percent blockade. **H.** Single order exponentials fitted to the average decay in the presence of MK-801 (left) and during the recovery (right) for each of the stimulation frequencies as indicated. 0.1 Hz data was fit to those cells presented in Figure 3. **I.** Percent of baseline blocked and percent of baseline recovered on average as a function of stimulation frequency. ** $p < 0.01$, *** $p < 0.005$.

NMDAR responses still recovered significantly following MK-801 blockade and washout (to 53 ± 7% of baseline values, $p < 0.05$ compared with the end of blockade), though to a lesser extent than with 0.1 Hz stimulation (Figure 3.4B-D). At 0.3 Hz (90 pulses), MK-801 blocked NMDAR EPSCs to 20 ± 7% of baseline, and EPSCs recovered 32 ± 6% of baseline, but the recovery was not significant ($p = 0.09$, Figure 3.4E-G). Increasing the stimulation frequency also increased the rate of the activity dependent decay in EPSC amplitudes following washout (Figure 3.4H, right). The increased blockade in both the 0.2 and 0.3 Hz conditions correlated with decreased recovery (Figure 3.4I). These data support a continuous lateral receptor movement between synaptic and extrasynaptic compartments, such that receptors potentially contributing to the recovery are blocked during MK-801 exposure.

3.3.4. NMDAR diffusion is not mediated by $[Ca^{2+}]_i$.

Given that NMDARs can be regulated by changes in the stimulation frequency, we next investigated the role of calcium. Intracellular calcium has been shown to regulate the trafficking of NMDARs to the surface [25, 51, 63] as well as NMDAR rundown [61]. We therefore predicted that intracellular calcium might play a role in the recovery. To this end, we repeated the 0.1 Hz MK-801 blockade experiment with BAPTA in the patch pipette. Surprisingly, neither 10 nor 15 mM BAPTA had any effect on the degree of blockade or recovery observed (Figure 3.5A and B).

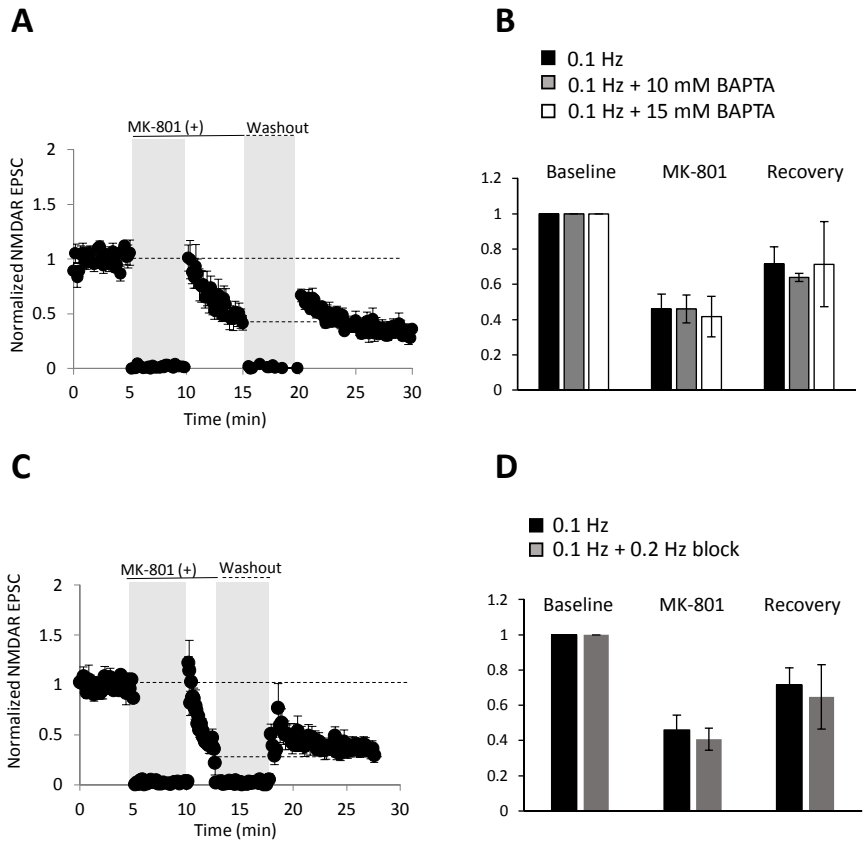

Figure 3.5 Recovery is not regulated by levels of intracellular calcium. **A.** Average peak NMDAR EPSC amplitude normalized to baseline with 10 mM BAPTA in the patch pipette (n =6). **B.** Quantification of NMDAR EPSC amplitudes during recovery experiment (Normal conditions, black bar (from Figure 3), 10 mM BAPTA, (gray bar, n = 6), 15 mM BAPTA (white bar, n =4). **C.** Average peak NMDAR EPSC amplitude normalized to baseline with increased frequency of block (n =6). **D.** Quantification of NMDAR amplitude as a percent of baseline (gray bar, n = 6) compared with normal conditions (black bar, from Figure 3).

To address whether it was the number of glutamate pulses delivered or the frequency at which the pulses were given, we doubled the frequency of stimulation during the MK-801 blockade, while cutting the blockade time in half, ultimately resulting in the same number of glutamate pulses delivered at twice the frequency. Should $[Ca^{2+}]_i$ participate in receptor mobility, increasing the stimulation frequency and the subsequent $[Ca^{2+}]_i$ accumulation should change both the rate of blockade and recovery following potentiation. We also saw no significant difference in this experiment, further indicative that $[Ca^{2+}]_i$ does not regulate this process (Figure 3.5C-D). Together, these results would suggest another activity-dependent, but calcium-independent mechanism governs receptor diffusion. We postulated that the binding of glutamate to NMDAR alone might be enough to induce a conformational change that promotes receptor movement out of synapses.

3.3.5. NMDAR diffusion is regulated by subunit composition.

NMDARs are heterotetramers, containing two obligatory GluN1 subunits and two GluN2-3 subunits, with the subunits the receptor contains conferring its kinetic and spatial properties. GluN2A-containing receptors demonstrate faster decay kinetics, and weak if any association with CaMKII, while GluN2B-containing receptors demonstrate slower decay kinetics, and tight association with CaMKII [21, 27]. The subunit composition of NMDARs located within synaptic vs. extrasynaptic zones has been a source of contention over the last decade, with a prevailing ideology that extrasynaptic receptors contain primarily GluN2B, and synaptic receptors GluN2A, though drawing definitive lines between the two has been complicated by the limitations of various experimental paradigms [104].

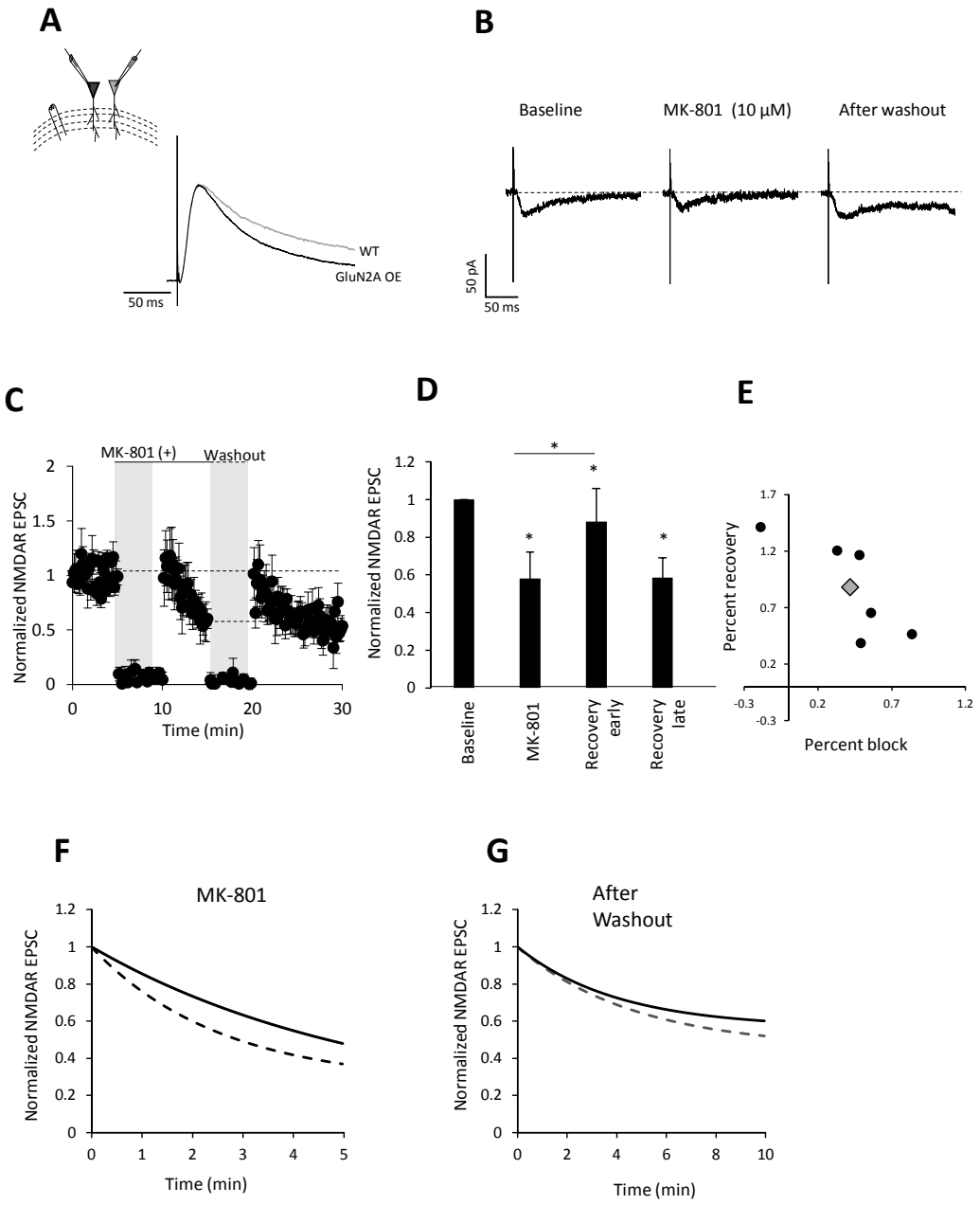

Figure 3.6 GluN2A overexpression does not prevent recovery. A. Sample traces of NMDAR EPSCs evoked from a cell overexpressing GluN2A-GFP and an adjacent wild type cell. These traces were acquired at +40 mV for maximal NMDAR activation. **B.** Sample NMDAR EPSCs acquired from cells overexpressing GluN2A-GFP at baseline, after 30 stimulus pulses in the presence of MK-801, and after washout. **C.** Average peak NMDAR EPSC amplitude normalized to baseline for recovery experiment (n = 6). **D.** Quantification of NMDAR EPSC amplitude compared to baseline at the times indicated. **E.** Percent of baseline recovered following washout as a function of percentage of baseline blocked. **F and G.** Single order exponential functions fit to the average NMDAR decay in the presence of MK-801 (**F**) and following washout (**G**). Dotted traces are from WT cells stimulated at 0.1 Hz (from Figure 4H). * $p < 0.05$.

The increase in the NMDAR EPSC time to half decay following MK-801 blockade (Figure 3.3C) suggests NMDAR diffusion is primarily mediated by GluN2B-containing receptors. Studies in cultured dissociated neurons distinguish GluN2B-containing receptors as more mobile than their GluN2A counterparts [100]. We therefore tested whether subunit composition had any role in either the blockade or recovery that we observed.

First, we overexpressed GluN2A-GFP and equimolar amounts of GluN1-GFP in organotypic hippocampal slices via biolistic transfection. Because GluN2A-containing receptors are considered more stable than their GluN2B counterparts, and thus receptors would not be able to escape synaptic block, we predicted that GluN2A overexpression would result in a fast decay in EPSC amplitudes during MK-801 exposure. We also predicted that there would be decreased recovery after washout. In this experiment, endogenous levels of GluN2B were left intact. Cells overexpressing the GluN2A construct were identified using the GFP tag. NMDAR-mediated currents evoked from these cells held at +40 mV demonstrated shorter time constants of decay than adjacent wildtype cells in the same slice, consistent with an increased GluN2A/GluN2B ratio (Figure 3.6A).

Contrary to our predictions, MK-801 blocked NMDAR EPSCs to only 58 ± 13% of baseline levels in these cells. A robust recovery was also observed (88 ± 17%, $p < 0.05$ compared with the end of blockade) almost achieving baseline levels, which is consistent with our previous results that decreased blockade allows for better recovery (Figure 3.6C-E). The rate of blockade via MK-801 was also slowed (Figure 3.6F).

The lesser extent of the MK-801 blockade observed in GluN2A expressing cells when compared to our previous experiments may be related a decreased efficiency of MK-801 for blocking GluN2A than GluN2B. This may be due to the relatively faster decay kinetics of the

GluN2A subunits. Since endogenous levels of GluN2B-containing receptors were intact, responses might still be able to recover. We concluded from this experiment that heightened expression of GluN2A subunits at least does not preclude recovery.

If increased expression of GluN2A does not prevent recovery only because GluN2B-containing receptors are still available to move into synapses, then eliminating GluN2B receptors should prevent recovery. To eliminate endogenous GluN2B, we used the subunit specific inhibitor, Ro 25-6981 (1 μM). Due to the activity dependence of this antagonist [111] we acquired a baseline of relatively large amplitude (50 – 100 pA) before adding Ro 25-6981. Fifteen minutes of Ro 25-6981 treatment at 0.1 Hz stimulation reduced NMDAR EPSCs to 57 ± 9% of baseline values (Figure 3.7A and C). From there, we repeated the MK-801 blockade paradigm. MK-801 blockade for 5 minutes decreased EPSCs to 33 ± 6% of baseline amplitude after Ro 25-6981 treatment. Following washout, responses did recover to 50 ± 8% on average, but it was not significant when compared to the end of the blockade ($p = 0.09$) and the response amplitudes decayed quickly (Figure 3.7B, D and E). Furthermore, Ro 25-6981 treatment before beginning the paradigm disrupted the correlation between percentage block and percent recovery ($R^2 = 0.12$, Figure 3.7F).

In combination, these data support that GluN2B-containing receptors are primarily responsible for the recovery observed after MK-801 block.

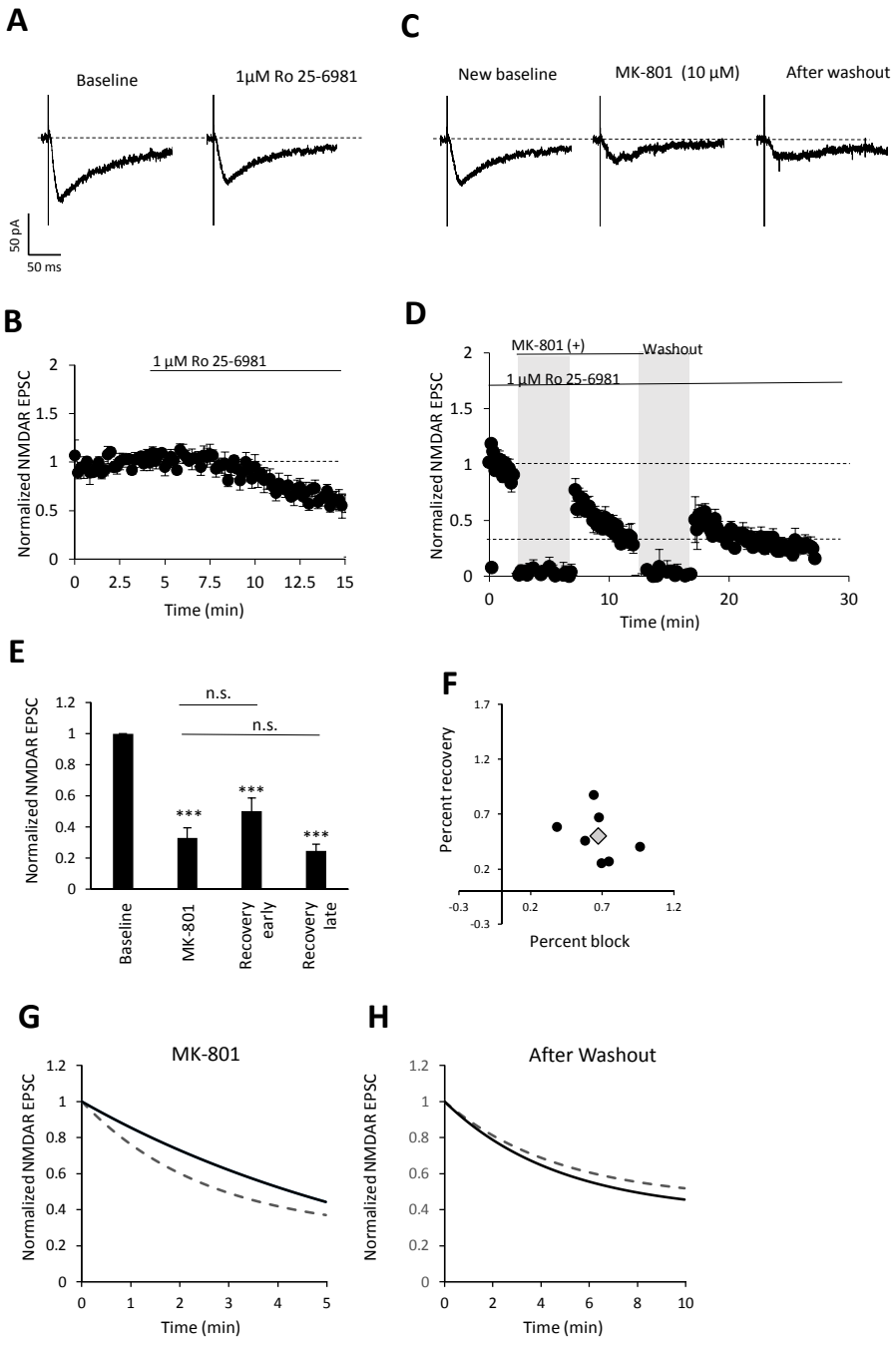

Figure 3.7 Pharmacological inhibition of GluN2B prevents recovery. **A.** Sample NMDAR EPSCs evoked at baseline and after 10-minutes treatment with Ro 25-6981. **B.** Average peak NMDAR EPSC at baseline and in the presence of 1μM Ro 25-6981 normalized to baseline. **C**. Sample NMDAR EPSCs evoked after ten minutes Ro 25-6981 treatment (same trace as in A), after 30 stimulus pulses in the presence of MK-801, and after washout. **D.** Average peak NMDAR EPSC amplitude normalized to the last three minutes in the presence of Ro 25-6981 before washing in the MK-801. Otherwise, same experiment as in Figure 3B (n =7). **E.** Quantification of NMDAR peak amplitude at the times indicated compared with the last three minutes of currents in the presence of Ro 25-6981. **F.** Percent of baseline recovered following washout as a function of percentage of baseline blocked. **G and H.** Single order exponential functions fit to the average decay in the presence of MK-801 (**G**) and after washout (**H**). Dotted traces are from WT cells stimulated at 0.1 Hz (from Figure 4H). *** $p < 0.005$

3.4. Discussion

We have demonstrated here that NMDAR can be rapidly and bidirectionally modified by activity, and that NMDAR EPSCs can recover following MK-801 synaptic block and a period of silence. This may be attributable to NMDAR lateral movement between synaptic and extrasynaptic sites, which is regulated by activity but not intracellular calcium. Our results lead us to a model where NMDARs, primarily those containing the GluN2B subunit, diffuse readily on the surface of neurons. In the absence of activity, they are more likely to stop in a synaptic domain and associate with MAGUK scaffolding proteins. NMDAR binding glutamate releases it from scaffolding, and promotes return of the receptor to the diffusible pool. Under constant stimulation, receptors reach an equilibrium of movement between synaptic and extrasynaptic spaces that results in a stable number of receptors within synapses (Figure 3.8).

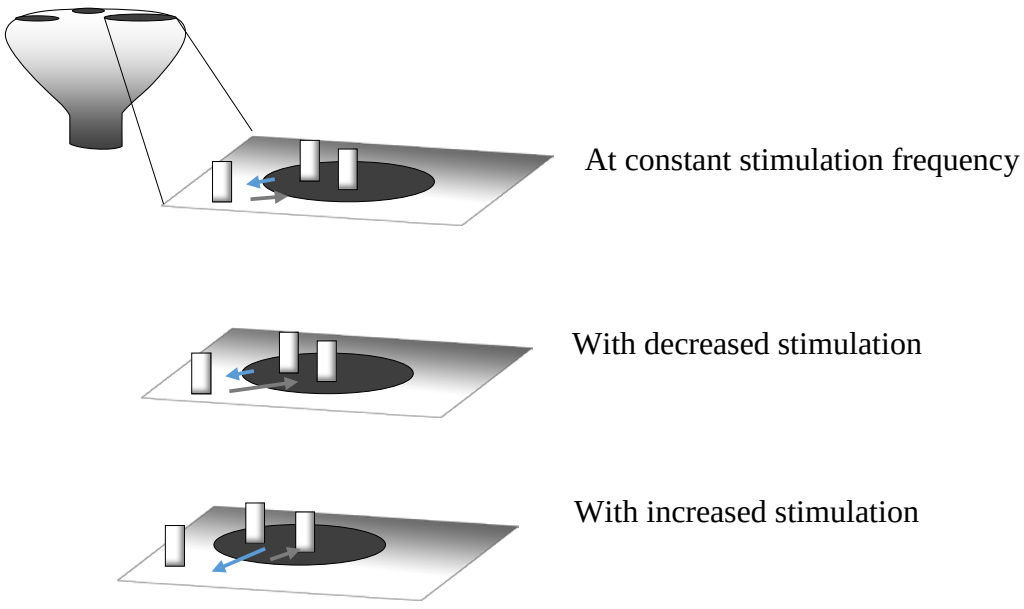

Figure 3.8 Proposed model of NMDAR diffusion. At a given level of stimulation, NMDARs diffuse into and out of synaptic domains at an activity-dependent equilibrium (top). Decreasing the stimulation frequency or the absence of stimulation can bias the equilibrium towards the presence of NMDARs in the synaptic site (middle). In contrast, increasing the stimulation frequency will bias the equilibrium towards the movement of NMDARs away from synapses (bottom).

If it is assumed that receptors can occupy either two discrete spaces, synaptic and extrasynaptic, then one simple way to describe this movement is to equate the change in the probability that the NMDAR will occupy the synapse to the difference between the rate of entering the synapse and the rate of leaving the synapse. That is:

$$\frac{dr}{dt} = \alpha_r(f)(1-r) - \beta_r(f)r \qquad \textit{eq. 3.1}$$

Where *r* represents the probability that a receptor will occupy the synapse, *f* is the stimulation frequency (or exposure to glutamate), α is the rate of receptors moving into the synapse, and β the rate of receptors moving away from a synapse. The terms 1-*r* and *r* represent the probability receptors in a given period of time are located extrasynaptically or in the synapse, respectively. Note that α and β are both independent functions of the stimulation frequency, such that increasing the stimulation frequency could lead to higher values of β and/or lower values of α, until a new equilibrium is reached. Decreasing the stimulation frequency would be predicted to have the opposite effect on these rates. In a simple computational simulation of MK-801 blockade that inlcudes both mobile and fixed receptor populations, solving this differential with constant values of α and β yields data similar to those acquired in Figure3.2A-C (model data not shown).

An alternative to this hypothesis is that silence leads to a modification, such as receptor phosphorylation, that increases channel open time, and this is the mechanism contributing to the increased NMDAR EPSC amplitude following synaptic MK-801 block. Because in our recovery experiments, we are not blocking all synaptic NMDARs, this is a real possibility. However, we

would still expect NMDAR-mediated EPSCs to be completely eliminated following extended exposure to MK-801, and this was not the case (Figure 3.2).

It is also possible that the failure to achieve complete blockade after 60 pulses of MK-801 (Figure 3.2) might be because of glutamate spillover during each stimulus pulse that could activate fixed extrasynaptic receptors. If this were the case, however, we would not expect an increase in that population following a period of silence, as in Figure 3.3.

Another possibility is that MK-801 unbinding from NMDAR during the silent period could account for the observed recovery. Although MK-801 is considered irreversible, there are reports stating that MK-801 can dissociate from receptor if the pore is open [105]. Since NMDARs close with MK-801 bound, NMDAR require binding glutamate in order for the MK-801 to dissociate. In our paradigm, this would lead to an increase in NMDAR-mediated currents once stimulation was resumed for the recovery phase. We, however, see an activity-dependent decrease in NMDAR-mediated currents, pointing against MK-801 unbinding as the mechanism behind the recovery.

The discrepancies between the results obtained here and those suggesting that NMDARs form stable synaptic and extrasynaptic pools in intact systems may be related to differences in MK-801 concentration, and the duration of exposure. For the majority of the experiments here, we used a relatively low MK-801concentration (10 μM), for a short duration and deliberately avoided inhibiting all receptors, since they are needed to contribute to the observed recovery. It is also possible that synapses on spines are not homogenous, but rather a collection of synaptic nanoscaffolding domains, where it has been shown that AMPAR are concentrated [112], such that inhibiting all NMDARs on a spine head could block recovery carried by receptors moving between domains.

The mechanism by which glutamate binding results in movement of receptors away from synapses also warrants further study. A calcium-independent metabotropic function of NMDARs has only recently come to light, whereby glutamate binding stimulates movement of the NMDAR C-terminus and changes receptor signaling properties [46, 49]. It is possible glutamate binding could also trigger a conformational change in receptor to promote diffusion away from synapses.

Taken together, this work supports a body of literature supporting the ability of NMDARs to diffuse between the synaptic and extrasynaptic spaces on a short time scale. This ability of NMDARs might control the GluN2B content of synapses and modify the ability of synapses to undergo potentiation or depression on a minute-by-minute basis. Full understanding of processes that regulate NMDARs will help develop novel therapeutics for neuropathologies where the ability of these receptors to coordinate plasticity has gone awry.

CHAPTER 4. CONCLUSION

I have shown in this work that synaptic NMDARs can be regulated acutely via two separate mechanisms that both impact receptor mobility, in support of a body of literature supporting that NMDARs can be dynamically regulated like their AMPAR counterparts.

In the second chapter, I demonstrated that Wnt5a can promote the delivery of new GluN2B-containing receptors into synapses. This trafficking was mediated by calcium release from the intracellular stores of neurons, which is initiated by membrane depolarization and the opening of voltage-gated calcium channels. This novel wnt/calcium signaling cascade in mature hippocampal neurons details a molecular mechanism by which neurons continue to regulate synaptic NMDAR content over the course of an organism's lifetime.

In the third chapter, by using the activity-dependent NMDAR antagonist, MK-801, I demonstrated that NMDARs could diffuse laterally into and out of synapses. This has previously has not been demonstrated in the physiological paradigm of the hippocampal slice, and supports that synapses can regulate their NMDAR content on a minute-by-minute basis through the diffusion between synaptic and extrasynaptic compartments. Evidence here suggests this mechanism is regulated by activity, but not intracellular calcium. Both of these mechanisms can increase the number of NMDARs within a synapse, shaping the EPSC, and therefore regulating the ability of that synapse to undergo plasticity.

In addition, both mechanisms point to the role of the GluN2B subunit as a primary contributor to this mobility. Given the constitutive nature of GluN2B trafficking [24], its ability to pass greater amounts of calcium than GluN2A-containingreceptors [21], and its association with CaMKII [27], if these mechanisms do increase levels of GluN2B, they are likely to have a significant impact on plasticity. The work also demonstrates that mobility, both in forward

trafficking (Chapter 2) and lateral diffusion (Chapter 3) of the GluN2B subunit persists in mature animals, and could be important for maintaining plasticity following the critical period and development. These detailed analyses of NMDAR dynamism on two different time scales challenges the notion that NMDARs are static components of synapses.

The studies shown here are concerned with NMDAR mobility, which is by far not the only means of regulating synaptic NMDAR. For example, receptors could be phosphorylated on their C termini to change channel open probabilities, or be subject to extracellular allosteric modulation. New roles and functions for NMDARs in neuronal physiology are also emerging. Thus, while these studies begin to elucidate a platform on which novel therapeutics might be developed, a deeper understanding of these receptors and how precisely they can be modified on specific time scales will be necessary for truly understanding neurodegenerative and other neuropsychiatric disorders.

This work exemplifies that the adult human brain is intrinsically plastic; both individual neurons and the brain as a whole contain mechanisms to ensure that proper changes in connectivity can occur in response to the external or internal environment throughout one's lifetime. This plasticity allows us the ability to change the way we see ourselves, and the realities we inhabit.

REFERENCES

1. Scoville, W. and B. Milner, *LOSS OF RECENT MEMORY AFTER BILATERAL HIPPOCAMPAL LESIONS.* Journal of Neurology, Neurosurgery & Psychiatry, 1957. **20**(1): p. 11-21.
2. Burgess, N., E.A. Maguire, and J. O'Keefe, *The human hippocampus and spatial and episodic memory.* Neuron, 2002. **35**(4): p. 625-41.
3. Fanselow, M. and H. Dong, *Are the Dorsal and Ventral Hippocampus Functionally Distinct Structures?* Neuron, 2010. **65**(1): p. 7-19.
4. Di Carlo, M., D. Giacomazza, and P.L. San Biagio, *Alzheimer's disease: biological aspects, therapeutic perspectives and diagnostic tools.* J Phys Condens Matter, 2012. **24**(24): p. 244102.
5. Bliss, T.V. and T. Lomo, *Long-lasting potentiation of synaptic transmission in the dentate area of the anaesthetized rabbit following stimulation of the perforant path.* J Physiol (Lond), 1973. **232**(2): p. 331-56.
6. Dudek, S.M. and M.F. Bear, *Homosynaptic long-term depression in area CA1 of hippocampus and effects of N-methyl-D-aspartate receptor blockade.* Proc Natl Acad Sci USA, 1992. **89**(10): p. 4363-7.
7. Malenka, R., *Long-Term Potentiation--A Decade of Progress?* Science, 1999. **285**(5435): p. 1870-1874.
8. Jahr, C.E. and C.F. Stevens, *Calcium permeability of the N-methyl-D-aspartate receptor channel in hippocampal neurons in culture.* Proc Natl Acad Sci USA, 1993. **90**(24): p. 11573-7.
9. Shi, S., *Rapid Spine Delivery and Redistribution of AMPA Receptors After Synaptic NMDA Receptor Activation.* Science, 1999. **284**(5421): p. 1811-1816.
10. Lisman, J., H. Schulman, and H. Cline, *The molecular basis of CaMKII function in synaptic and behavioural memory.* Nat Rev Neurosci, 2002. **3**(3): p. 175-90.
11. Yang, S.N., Y.G. Tang, and R.S. Zucker, *Selective induction of LTP and LTD by postsynaptic [Ca2+]i elevation.* Journal of Neurophysiology, 1999. **81**(2): p. 781-7.
12. Matsuzaki, M., et al., *Structural basis of long-term potentiation in single dendritic spines.* Nature, 2004. **429**(6993): p. 761-6.
13. Collingridge, G.L., S.J. Kehl, and H. McLennan, *Excitatory amino acids in synaptic transmission in the Schaffer collateral-commissural pathway of the rat hippocampus.* J Physiol (Lond), 1983. **334**: p. 33-46.
14. Morris, R.G., et al., *Selective impairment of learning and blockade of long-term potentiation by an N-methyl-D-aspartate receptor antagonist, AP5.* Nature, 1986. **319**(6056): p. 774-6.
15. Tsien, J.Z., P.T. Huerta, and S. Tonegawa, *The essential role of hippocampal CA1 NMDA receptor-dependent synaptic plasticity in spatial memory.* Cell, 1996. **87**(7): p. 1327-38.
16. Monaghan, D.T. and C.W. Cotman, *Distribution of N-methyl-D-aspartate-sensitive L-[3H]glutamate-binding sites in rat brain.* J Neurosci, 1985. **5**(11): p. 2909-19.
17. Bliss, T.V. and G.L. Collingridge, *A synaptic model of memory: long-term potentiation in the hippocampus.* Nature, 1993. **361**(6407): p. 31-9.
18. Traynelis, S., et al., *Glutamate Receptor Ion Channels: Structure, Regulation, and Function.* Pharmacological Reviews, 2010. **62**(3): p. 405-496.

19. Paoletti, P., C. Bellone, and Q. Zhou, *NMDA receptor subunit diversity: impact on receptor properties, synaptic plasticity and disease.* Nat Rev Neurosci, 2013. **14**(6): p. 383-400.
20. Sanz-Clemente, A., R. Nicoll, and K. Roche, *Diversity in NMDA Receptor Composition: Many Regulators, Many Consequences.* The Neuroscientist, 2013. **19**(1): p. 62-75.
21. Vicini, S., et al., *Functional and pharmacological differences between recombinant N-methyl-D-aspartate receptors.* Journal of Neurophysiology, 1998. **79**(2): p. 555-66.
22. Lau, C., et al., *SNAP-25 Is a Target of Protein Kinase C Phosphorylation Critical to NMDA Receptor Trafficking.* Journal of Neuroscience, 2010. **30**(1): p. 242-254.
23. Lavezzari, G., et al., *Differential binding of the AP-2 adaptor complex and PSD-95 to the C-terminus of the NMDA receptor subunit NR2B regulates surface expression.* Neuropharmacology, 2003. **45**(6): p. 729-737.
24. Barria, A. and R. Malinow, *Subunit-specific NMDA receptor trafficking to synapses.* Neuron, 2002. **35**(2): p. 345-53.
25. Matta, J., et al., *mGluR5 and NMDA Receptors Drive the Experience- and Activity-Dependent NMDA Receptor NR2B to NR2A Subunit Switch.* Neuron, 2011. **70**(2): p. 339-351.
26. Lavezzari, G., *Subunit-Specific Regulation of NMDA Receptor Endocytosis.* Journal of Neuroscience, 2004. **24**(28): p. 6383-6391.
27. Barria, A. and R. Malinow, *NMDA Receptor Subunit Composition Controls Synaptic Plasticity by Regulating Binding to CaMKII.* Neuron, 2005. **48**(2): p. 289-301.
28. Sanz-Clemente, A., et al., *Casein Kinase 2 Regulates the NR2 Subunit Composition of Synaptic NMDA Receptors.* Neuron, 2010. **67**(6): p. 984-996.
29. Sanz-Clemente, A., et al., *Activated CaMKII Couples GluN2B and Casein Kinase 2 to Control Synaptic NMDA Receptors.* Cell Reports, 2013. **3**(3): p. 607-614.
30. Liu, L., *Role of NMDA Receptor Subtypes in Governing the Direction of Hippocampal Synaptic Plasticity.* Science, 2004. **304**(5673): p. 1021-1024.
31. Massey, P., *Differential Roles of NR2A and NR2B-Containing NMDA Receptors in Cortical Long-Term Potentiation and Long-Term Depression.* Journal of Neuroscience, 2004. **24**(36): p. 7821-7828.
32. Foster, K., et al., *Distinct Roles of NR2A and NR2B Cytoplasmic Tails in Long-Term Potentiation.* Journal of Neuroscience, 2010. **30**(7): p. 2676-2685.
33. Morishita, W., et al., *Activation of NR2B-containing NMDA receptors is not required for NMDA receptor-dependent long-term depression.* Neuropharmacology, 2007. **52**(1): p. 71-76.
34. Bienenstock, E.L., L.N. Cooper, and P.W. Munro, *Theory for the development of neuron selectivity: orientation specificity and binocular interaction in visual cortex.* J Neurosci, 1982. **2**(1): p. 32-48.
35. Cooper, L.N. and M. Bear, *The BCM theory of synapse modification at 30: interaction of theory with experiment.* Nat Rev Neurosci, 2012. **13**(11): p. 798-810.
36. Gambrill, A. and A. Barria, *NMDA receptor subunit composition controls synaptogenesis and synapse stabilization.* Proceedings of the National Academy of Sciences, 2011. **108**(14): p. 5855-5860.
37. Yashiro, K. and B. Philpot, *Regulation of NMDA receptor subunit expression and its implications for LTD, LTP, and metaplasticity.* Neuropharmacology, 2008. **55**(7): p. 1081-1094.

38. Quinlan, E.M., D.H. Olstein, and M.F. Bear, *Bidirectional, experience-dependent regulation of N-methyl-D-aspartate receptor subunit composition in the rat visual cortex during postnatal development.* Proc Natl Acad Sci USA, 1999. **96**(22): p. 12876-80.
39. Philpot, B.D., et al., *Visual experience and deprivation bidirectionally modify the composition and function of NMDA receptors in visual cortex.* Neuron, 2001. **29**(1): p. 157-69.
40. Sheng, M., et al., *Changing subunit composition of heteromeric NMDA receptors during development of rat cortex.* Nature, 1994. **368**(6467): p. 144-7.
41. Williams, K., et al., *Developmental switch in the expression of NMDA receptors occurs in vivo and in vitro.* Neuron, 1993. **10**(2): p. 267-78.
42. Quinlan, E.M., et al., *Rapid, experience-dependent expression of synaptic NMDA receptors in visual cortex in vivo.* Nat Neurosci, 1999. **2**(4): p. 352-7.
43. Bellone, C. and R. Nicoll, *Rapid Bidirectional Switching of Synaptic NMDA Receptors.* Neuron, 2007. **55**(5): p. 779-785.
44. Adesnik, H., et al., *NMDA receptors inhibit synapse unsilencing during brain development.* Proc Natl Acad Sci USA, 2008. **105**(14): p. 5597-602.
45. Gray, J., et al., *Distinct Modes of AMPA Receptor Suppression at Developing Synapses by GluN2A and GluN2B: Single-Cell NMDA Receptor Subunit Deletion In Vivo.* Neuron, 2011. **71**(6): p. 1085-1101.
46. Nabavi, S., et al., *Metabotropic NMDA receptor function is required for NMDA receptor-dependent long-term depression.* Proceedings of the National Academy of Sciences, 2013. **110**(10): p. 4027-4032.
47. Babiec, W., et al., *Ionotropic NMDA Receptor Signaling Is Required for the Induction of Long-Term Depression in the Mouse Hippocampal CA1 Region.* Journal of Neuroscience, 2014. **34**(15): p. 5285-5290.
48. Stein, I., J. Gray, and K. Zito, *Non-Ionotropic NMDA Receptor Signaling Drives Activity-Induced Dendritic Spine Shrinkage.* Journal of Neuroscience, 2015. **35**(35): p. 12303-12308.
49. Dore, K., J. Aow, and R. Malinow, *Agonist binding to the NMDA receptor drives movement of its cytoplasmic domain without ion flow.* Proc Natl Acad Sci USA, 2015. **112**(47): p. 14705-14710.
50. Aow, J., K. Dore, and R. Malinow, *Conformational signaling required for synaptic plasticity by the NMDA receptor complex.* Proc Natl Acad Sci USA, 2015. **112**(47): p. 14711-14716.
51. Lau, C. and R. Zukin, *NMDA receptor trafficking in synaptic plasticity and neuropsychiatric disorders.* Nat Rev Neurosci, 2007. **8**(6): p. 413-426.
52. Hanson, J., et al., *Altered GluN2B NMDA receptor function and synaptic plasticity during early pathology in the PS2APP mouse model of Alzheimer's disease.* Neurobiology of Disease, 2015. **74**: p. 254-262.
53. Thibault, O., R. Hadley, and P.W. Landfield, *Elevated postsynaptic [Ca2+]i and L-type calcium channel activity in aged hippocampal neurons: relationship to impaired synaptic plasticity.* J Neurosci, 2001. **21**(24): p. 9744-56.
54. Oh, M., et al., *Altered Calcium Metabolism in Aging CA1 Hippocampal Pyramidal Neurons.* Journal of Neuroscience, 2013. **33**(18): p. 7905-7911.

55. Danysz, W. and C. Parsons, *Alzheimer's disease, β-amyloid, glutamate, NMDA receptors and memantine - searching for the connections.* British Journal of Pharmacology, 2012. **167**(2): p. 324-352.
56. Kerchner, G. and R. Nicoll, *Silent synapses and the emergence of a postsynaptic mechanism for LTP.* Nat Rev Neurosci, 2008. **9**(11): p. 813-825.
57. Lissin, D.V., et al., *Activity differentially regulates the surface expression of synaptic AMPA and NMDA glutamate receptors.* Proc Natl Acad Sci USA, 1998. **95**(12): p. 7097-102.
58. Rao, A. and A.M. Craig, *Activity regulates the synaptic localization of the NMDA receptor in hippocampal neurons.* Neuron, 1997. **19**(4): p. 801-12.
59. Gambrill, A., G. Storey, and A. Barria, *Dynamic Regulation of NMDA Receptor Transmission.* Journal of Neurophysiology, 2011. **105**(1): p. 162-171.
60. Rosenmund, C. and G.L. Westbrook, *Calcium-induced actin depolymerization reduces NMDA channel activity.* Neuron, 1993. **10**(5): p. 805-14.
61. Rosenmund, C. and G.L. Westbrook, *Rundown of N-methyl-D-aspartate channels during whole-cell recording in rat hippocampal neurons: role of Ca2+ and ATP.* J Physiol (Lond), 1993. **470**: p. 705-29.
62. Legendre, P., C. Rosenmund, and G.L. Westbrook, *Inactivation of NMDA channels in cultured hippocampal neurons by intracellular calcium.* J Neurosci, 1993. **13**(2): p. 674-84.
63. Hunt, D., et al., *Bidirectional NMDA receptor plasticity controls CA3 output and heterosynaptic metaplasticity.* Nat Neurosci, 2013. **16**(8): p. 1049-1059.
64. Cerpa, W., et al., *Regulation of NMDA-Receptor Synaptic Transmission by Wnt Signaling.* Journal of Neuroscience, 2011. **31**(26): p. 9466-9471.
65. Cerpa, W., E. Latorre-Esteves, and A. Barria, *RoR2 functions as a noncanonical Wnt receptor that regulates NMDAR-mediated synaptic transmission.* Proc Natl Acad Sci USA, 2015. **112**(15): p. 4797-4802.
66. Angers, S. and R. Moon, *Proximal events in Wnt signal transduction.* Nat Rev Mol Cell Biol, 2009: p. 10.
67. Van Amerongen, R. and R. Nusse, *Towards an integrated view of Wnt signaling in development.* Development, 2009. **136**(19): p. 3205-3214.
68. Ciani, L. and P. Salinas, *Signalling in neural development: WNTS in the vertebrate nervous system: from patterning to neuronal connectivity.* Nat Rev Neurosci, 2005. **6**(5): p. 351-362.
69. Inestrosa, N. and E. Arenas, *Emerging roles of Wnts in the adult nervous system.* Nat Rev Neurosci, 2010. **11**(2): p. 77-86.
70. Mao, Y., et al., *Disrupted in Schizophrenia 1 Regulates Neuronal Progenitor Proliferation via Modulation of GSK3β/β-Catenin Signaling.* Cell, 2009. **136**(6): p. 1017-1031.
71. Zandi, P., *Association Study of Wnt Signaling Pathway Genes in Bipolar Disorder.* Arch Gen Psychiatry, 2008. **65**(7): p. 785.
72. Emamian, E., et al., *Convergent evidence for impaired AKT1-GSK3β signaling in schizophrenia.* Nat Genet, 2004. **36**(2): p. 131-137.
73. Caricasole, A., et al., *The Wnt pathway, cell-cycle activation and β-amyloid: novel therapeutic strategies in Alzheimer's disease?* Trends in Pharmacological Sciences, 2003. **24**(5): p. 233-238.

74. De Ferrari, G.V. and N.C. Inestrosa, *Wnt signaling function in Alzheimer's disease.* Brain Res Brain Res Rev, 2000. **33**(1): p. 1-12.
75. Anastas, J. and R. Moon, *WNT signalling pathways as therapeutic targets in cancer.* Nat Rev Cancer, 2012. **13**(1): p. 11-26.
76. Logan, C. and R. Nusse, *THE WNT SIGNALING PATHWAY IN DEVELOPMENT AND DISEASE.* Annu. Rev. Cell Dev. Biol., 2004. **20**(1): p. 781-810.
77. Van Amerongen, R., A. Mikels, and R. Nusse, *Alternative Wnt Signaling Is Initiated by Distinct Receptors.* Science Signaling, 2008. **1**(35): p. re9-re9.
78. Kohn, A. and R. Moon, *Wnt and calcium signaling: β-Catenin-independent pathways.* Cell Calcium, 2005. **38**(3-4): p. 439-446.
79. Veeman, M.T., J.D. Axelrod, and R. Moon, *A second canon. Functions and mechanisms of beta-catenin-independent Wnt signaling.* Dev Cell, 2003. **5**(3): p. 367-77.
80. Slusarski, D.C., V.G. Corces, and R.T. Moon, *Interaction of Wnt and a Frizzled homologue triggers G-protein-linked phosphatidylinositol signalling.* Nature, 1997. **390**(6658): p. 410-3.
81. Kuhl, M., *Ca2+/Calmodulin-dependent Protein Kinase II Is Stimulated by Wnt and Frizzled Homologs and Promotes Ventral Cell Fates in Xenopus.* Journal of Biological Chemistry, 2000. **275**(17): p. 12701-12711.
82. Sheldahl, L.C., et al., *Protein kinase C is differentially stimulated by Wnt and Frizzled homologs in a G-protein-dependent manner.* Curr Biol, 1999. **9**(13): p. 695-8.
83. Strutt, D., *Frizzled signalling and cell polarisation in Drosophilaand vertebrates.* Development, 2003. **130**(19): p. 4501-4513.
84. Cerpa, W., et al., *Wnt-7a modulates the synaptic vesicle cycle and synaptic transmission in hippocampal neurons.* J Biol Chem, 2008. **283**(9): p. 5918-27.
85. Salinas, P., *Wnt Signaling in the Vertebrate Central Nervous System: From Axon Guidance to Synaptic Function.* Cold Spring Harbor Perspectives in Biology, 2012. **4**(2): p. a008003-a008003.
86. Farias, G., et al., *Wnt-5a/JNK Signaling Promotes the Clustering of PSD-95 in Hippocampal Neurons.* Journal of Biological Chemistry, 2009. **284**(23): p. 15857-15866.
87. Varela-Nallar, L., et al., *Wingless-type family member 5A (Wnt-5a) stimulates synaptic differentiation and function of glutamatergic synapses.* Proceedings of the National Academy of Sciences, 2010. **107**(49): p. 21164-21169.
88. Opitz-Araya, X. and A. Barria, *Organotypic Hippocampal Slice Cultures.* JoVE, 2011(48): p. 3.
89. Plenge-Tellechea, F., F. Soler, and F. Fernandez-Belda, *On the Inhibition Mechanism of Sarcoplasmic or Endoplasmic Reticulum Ca2+-ATPases by Cyclopiazonic Acid.* Journal of Biological Chemistry, 1997. **272**(5): p. 2794-2800.
90. Berridge, M., *The Inositol Trisphosphate/Calcium Signaling Pathway in Health and Disease.* Physiol Rev, 2016. **96**(4): p. 1261-1296.
91. Poolos, N., M. Migliore, and D. Johnston, *Pharmacological upregulation of h-channels reduces the excitability of pyramidal neuron dendrites.* Nat Neurosci, 2002: p. 8.
92. Miesenböck, G., D.A. De Angelis, and J.E. Rothman, *Visualizing secretion and synaptic transmission with pH-sensitive green fluorescent proteins.* Nature, 1998. **394**(6689): p. 192-5.
93. Kennedy, M., et al., *Syntaxin-4 Defines a Domain for Activity-Dependent Exocytosis in Dendritic Spines.* Cell, 2010. **141**(3): p. 524-535.

94. Kani, S., et al., *The receptor tyrosine kinase Ror2 associates with and is activated by casein kinase Iepsilon.* J Biol Chem, 2004. **279**(48): p. 50102-9.
95. Mikels, A., Y. Minami, and R. Nusse, *Ror2 Receptor Requires Tyrosine Kinase Activity to Mediate Wnt5A Signaling.* Journal of Biological Chemistry, 2009. **284**(44): p. 30167-30176.
96. Shimogori, T., et al., *Members of theWnt,Fz, andFrp gene families expressed in postnatal mouse cerebral cortex.* J. Comp. Neurol., 2004. **473**(4): p. 496-510.
97. Lein, E., et al., *Genome-wide atlas of gene expression in the adult mouse brain.* Nature, 2007. **445**(7124): p. 168-176.
98. Paganoni, S., J. Bernstein, and A. Ferreira, *Ror1-Ror2 complexes modulate synapse formation in hippocampal neurons.* Neuroscience, 2010. **165**(4): p. 1261-1274.
99. Suh, B. and B. Hille, *Regulation of KCNQ channels by manipulation of phosphoinositides.* The Journal of Physiology, 2007. **582**(3): p. 911-916.
100. Groc, L., et al., *NMDA receptor surface mobility depends on NR2A-2B subunits.* Proc Natl Acad Sci USA, 2006. **103**(49): p. 18769-74.
101. Malinow, R. and R. Malenka, *AMPA receptor trafficking and synaptic plasticity.* Annu. Rev. Neurosci., 2002. **25**: p. 103-26.
102. Chung, H., *Regulation of the NMDA Receptor Complex and Trafficking by Activity-Dependent Phosphorylation of the NR2B Subunit PDZ Ligand.* Journal of Neuroscience, 2004. **24**(45): p. 10248-10259.
103. Hardingham, G. and H. Bading, *Synaptic versus extrasynaptic NMDA receptor signalling: implications for neurodegenerative disorders.* Nat Rev Neurosci, 2010. **11**(10): p. 682-696.
104. Papouin, T. and S.H. Oliet, *Organization, control and function of extrasynaptic NMDA receptors.* Philos Trans R Soc Lond, B, Biol Sci, 2014. **369**(1654): p. 20130601.
105. Tovar, K.R. and G.L. Westbrook, *Mobile NMDA receptors at hippocampal synapses.* Neuron, 2002. **34**(2): p. 255-64.
106. Groc, L., et al., *Differential activity-dependent regulation of the lateral mobilities of AMPA and NMDA receptors.* Nat Neurosci, 2004. **7**(7): p. 695-696.
107. Harris, A. and D. Pettit, *Extrasynaptic and synaptic NMDA receptors form stable and uniform pools in rat hippocampal slices.* The Journal of Physiology, 2007. **584**(2): p. 509-519.
108. Wamil, A.W. and M.J. McLean, *Use-, concentration- and voltage-dependent limitation by MK-801 of action potential firing frequency in mouse central neurons in cell culture.* J Pharmacol Exp Ther, 1992. **260**(1): p. 376-83.
109. Snell, L.D., S.J. Yi, and K.M. Johnson, *Comparison of the effects of MK-801 and phencyclidine on catecholamine uptake and NMDA-induced norepinephrine release.* Eur J Pharmacol, 1988. **145**(2): p. 223-6.
110. Hessler, N.A., A.M. Shirke, and R. Malinow, *The probability of transmitter release at a mammalian central synapse.* Nature, 1993. **366**(6455): p. 569-72.
111. Kew, J.N., G. Trube, and J.A. Kemp, *A novel mechanism of activity-dependent NMDA receptor antagonism describes the effect of ifenprodil in rat cultured cortical neurones.* J Physiol (Lond), 1996. **497 (Pt 3)**: p. 761-72.
112. Macgillavry, H., et al., *Nanoscale Scaffolding Domains within the Postsynaptic Density Concentrate Synaptic AMPA Receptors.* Neuron, 2013. **78**(4): p. 615-622.

VITA

Andrea McQuate is from the Bay Area, northern California. She graduated from Oberlin College in 2010 with a degree in neuroscience, minors in chemistry and East Asian Studies. During that time, she began researching glutamate receptors, and how their kinetic properties could shape synaptic transmission in the hippocampus in a collaborative project with Dr. Kathryn Partin at Colorado State University. After graduating, she joined the lab of Dr. Xinyu Zhao at the Univeristy of New Mexico, studying the role epigenetics in determining neural stem cell fate during adult neurogenesis. She began graduate school at the University of Washington in 2011.